Poultry Science

Establishment and characterization of an SV40 immortalized chicken intestinal epithelial cell line

Federico Ghiselli [*], Martina Felici [†], Andrea Piva,[*,†] and Ester Grilli[†,‡,1]

[*]*Vetagro S.p.A., Reggio Emilia 42124, Italy;* [†]*DIMEVET, Ozzano dell'Emilia (BO) - University of Bologna, Bologna 40064, Italy; and* [‡]*Vetagro Inc., Chicago, IL 60603, USA*

ABSTRACT Primary chicken intestinal epithelial cells or 3D enteroids are a powerful tool to study the different biological mechanisms that occur in the chicken intestine. Unfortunately, they are not ideal for large-scale screening or long-term studies due to their short lifespan. Moreover, they require expensive culture media, coatings, or the usage of live embryos for each isolation. The aim of this study was to establish and characterize an immortalized chicken intestinal epithelial cell line to help the study of host−pathogen interactions in poultry. This cell line was established by transducing into primary chicken enterocytes the SV40 large-T antigen through a lentiviral vector. The transduced cells grew without changes up to 40 passages maintaining, after a differentiation phase of 48 h with epidermal growth factor, the biological properties of mature enterocytes such as alkaline phosphatase activity and tight junction formation. Immortalized enterocytes were able to generate a cytokine response during an inflammatory challenge, and showed to be susceptible to *Eimeria tenella* sporozoites invasion and generate a proper immune response to parasitic and lipopolysaccharide (*Escherichia coli*) stimulation. This immortalized cell line could be a cost-effective and easy-to-maintain model for all the public health, food safety, or research and pharmaceutical laboratories that study host−pathogen interactions, foodborne pathogens, and food or feed science in vitro.

Key words: chicken enterocyte, immortalization, epithelial cell, SV40, host−pathogen model

2023 Poultry Science 102:102864
https://doi.org/10.1016/j.psj.2023.102864

INTRODUCTION

Avian research is crucial for the global economy. Over the past 20 years, poultry production has increased 3-fold, resulting in 107 million tons of chicken meat and 1.3 trillion eggs produced annually, with projections of continued growth in emerging countries (FAOSTAT, 2018). The spread of diseases like avian influenza, *Salmonella spp.*, *C. perfringens*, and other foodborne pathogens pose a threat to public health, while parasites like *Eimeria spp.* harm animal welfare and poultry production yields. A lack of representative cell culture models has hindered in vitro studies of the avian gut and pathogens (Ghiselli et al., 2021b).

Intestinal epithelial cells are the main entry site for nutrients and pathogens inside the body (Maynard et al., 2012). Those cells are really important for food absorption and initiate the innate immune response against pathogens (Bar Shira and Friedman, 2018). In literature, different methods to isolate and obtain primary chicken intestinal epithelial cells (**cIEC**) are present (Dimier-Poisson et al., 2004; Byrne et al., 2007; Kaiser et al., 2017; Bar Shira and Friedman, 2018; Bussière et al., 2018; Rath et al., 2018; Orr et al., 2021; Ghiselli et al., 2021a). Unfortunately, those models require fresh live embryos for each isolation and none of them is capable to propagate for many passages without losing some of their crucial aspects. Also, they often require expensive coatings or complex culture media to be maintained in culture for up to 10 to 12 d (Ghiselli et al., 2021a). Three-dimensional enteroids are another interesting chicken in vitro model. In 2012, Pierzchalska and colleagues published for the first time the development of chicken embryo intestinal organoids in Matrigel matrix (Pierzchalska et al., 2012). Recently, Oost et al. (2022) showed that chicken intestinal organoids can be cultured for multiple passages using chicken-derived WNT3 and RSPO1, prostaglandin E2, and forkhead box O1-inhibitor (Oost et al., 2022). Those are wonderful models but as primary cells they require the usage of Matrigel and expensive growth factors to be passaged and maintained for 15 passages. In 2021, Nash et al. published a detailed method to culture apical-out chicken organoids. They created a comprehensive model

Received April 10, 2023.
Accepted June 8, 2023.

[1]Corresponding author: ester.grilli@unibo.it

of the chicken intestine that contains both the epithelial and leucocyte components that can be maintained in a cheaper culture medium (Nash et al., 2021). These apical-out organoids are the closest in vitro model to the chicken live intestine but they require live animals for the isolations to survive only 7 to 9 d in culture. Moreover, they reported that there was no postpassage growth or budding of these enteroids (Nash et al., 2021).

For those reasons, primary cells or 3D enteroids are not suitable for large or routine screenings or long-term studies. Moreover, at the time of publication, no other immortalized cIEC cell line was already established and fully characterized, to our knowledge. Two avian intestinal cell lines are commercially available, an SV40-immortalized embryonic line (Accegen) and a clonal line (CHIC-8E11). The SV40-immortalized line, although available for purchase, has never been used in scientific publications to our knowledge, and detailed information regarding its characteristics is currently lacking. On the other hand, the 8E11 clone has been used in some published studies (John et al., 2017; Han and Bertzbach, 2019; Ali et al., 2020; Kolenda et al., 2021) but it lacks a comprehensive and detailed characterization required for validating its suitability as a research model.

Large-T antigen is a transforming protein that inhibits p53 action, thus inducing cell replication (Manfredi and Prives, 1994; Sheppard et al., 1999). SV40 has been already used to immortalize chicken fibroblasts, for example (patent US10428316B2).

The aim of this study was to develop and fully characterize a cIEC immortalized cell line suitable to expand over time and maintain the functional characteristics of freshly isolated enterocytes. The establishment and characterization of an immortalized intestinal cell line could help to study intestinal health and all the interactions with chicken intestinal pathogens, enteric viruses, and foodborne pathogens in vitro. Moreover, they could guarantee a cost-effective and easy-to-maintain model for all the public health, food safety, or research laboratories that study chicken intestinal epithelium and chicken cells in health and disease.

MATERIAL AND METHODS

Care and Use of Animals

Specific pathogen-free eggs were purchased from Valo-Biomedia (Osterholz-Scharmbeck, Germany) and incubated at 37.7°C, 48% relative humidity in a semi-automated incubator. On the 19th day of incubation, according to the AVMA guidelines and animal welfare, chick embryos were sacrificed by decapitation. As chick embryos older than 14 d can experience pain, decapitation was recommended as a humane method of euthanasia. According to the Italian legislation (D.lgs. 26/2014, the act on the protection of animals used for scientific and educational purposes, which was passed in March 2014 and transposed Directive 2010/63/EU into current Italian legislation), avian embryos are not considered as "live vertebrate animals," so the approval of Animal Ethics Commission was not required.

Cell Immortalization

For all the experiments involving primary cells and for immortalization, cIEC were isolated using the method reported by Ghiselli and colleagues (Ghiselli et al., 2021a). The obtained cell aggregates were seeded on 35 mm petri dishes (30,000 aggregates/dish—Cat. # 353001—Corning Incorporated, Corning, NY) coated with Matrigel matrix (Cat. # 356234—Corning Incorporated) diluted at the final concentration of 0.8 mg/mL. Cells were cultured with the proper isolation medium, reported in Table 1, for 24 h at 37°C and 5% CO_2. After the first expansion, primary cells were incubated in an immortalization medium as indicated in Table 1, for another 24 h with an SV40 T-antigen VSV-G lentiviral vector (Cat.# CILV01—ALSTEM, Richmond, CA), following the manufacturer instructions in presence of transplus virus transduction enhancer (Cat.# V020—ALSTEM, Richmond, CA). Supplementary Figure 1 represents the construct used for transduction.

After transduction, cells were washed with Hank's balanced salt solution without magnesium and chloride (Cat.# 55021C—Sigma-Aldrich, St. Louis, MO), and

Table 1. Recipes of different media used during the immortalization protocol.

Media	Composition
Isolation medium	• Dulbecco modified eagle's medium high glucose (Cat. # D1145—Sigma-Aldrich). • 2% fetal bovine serum (Cat. # F7524—Sigma-Aldrich). • 1x penicillin-streptomycin (Cat. # P4333—Sigma-Aldrich). • 2 mM L-glutamine (Cat. # G7513—Sigma-Aldrich). • 1x ITS premix (Cat. # 354350 Corning Incorporated). • 25 ng/mL mouse recombinant epidermal growth factor (mEGF—Cat. # SRP3196—Sigma-Aldrich). • 1 mM sodium pyruvate (Cat. # P5280—Sigma-Aldrich). • 0.1 mg/mL heparin sodium salt from intestinal porcine mucosa (Cat. # H3149—Sigma-Aldrich). • 1× nonessential amino acids (Cat. # X0557—VWR, www.wvr.com). • 1 mM sodium butyrate (Cat. # B103500—Sigma-Aldrich). • 0.081 mg/L putrescine (Cat. # P5780—Sigma-Aldrich). • 10 mM 4-(2-hydroxyethyl)-1-piperazineethanesulfonic acid) (HEPES—Cat. # H4034—Sigma-Aldrich). • 10 μM Y-27632 (Cat.# Y0503—Sigma-Aldrich).
Immortalization medium	• Dulbecco modified eagle's medium high glucose • 2 mM L-glutamine • 1× ITS premix • 1× nonessential amino acids • 25 ng/mL mEGF • 1 mM sodium pyruvate • 10 mM HEPES
Expansion medium	• Dulbecco modified eagle's medium high glucose • 10% fetal bovine serum • 1× penicillin-streptomycin • 2 mM L-glutamine • 1× nonessential amino acids • 1 mM sodium pyruvate • 10 mM HEPES

cultured for 48 h in an isolation medium (Table 1). Then, transduced cells were detached and monoclonal selection were performed using a limiting dilution method seeding one cell per well in a Matrigel-coated 96-well plate (Cat. # 353072—Corning Incorporated). Then, clones that showed proliferation in the first 24 h were positively selected using an expansion medium (Table 1) added with 4 ppm of puromycin dihydrochloride (Cat.# HY-B1743A—MedChemExpress, South Brunswick, NJ) for 14 d. The concentration of puromycin was chosen based on a previous kill curve assay performed on cIEC (Supplementary Figure 2a). To assess the correct viral transduction, the kill curve was then performed again on the immortalized cells to assess the presence of puromycin resistance (Supplementary Figure 2b). From this selection, 3 clones were generated but 2 of them undergone senescence before reaching confluence.

Culture Conditions and Differentiation

Once the remaining transduced clone reached confluency, cells (named from now on **cIEC-H2**) were detached using Accutase (Cat.# 25-058-CI- Corning Incorporated) and all the obtained cells (around 75,000 cells) were seeded on a T-25 flask (3,000 cells/cm^2—Cat.# 83.3910.300 SARSTEDT AG & Co. KG, Germany) using the same expansion medium added with 4 ppm of puromycin. After 13 d, cells reached again confluency and they were then detached with Accutase (obtained around 930,000 cells) and moved onto a T-75 flask (12,400 cells/cm^2—Cat.# 83.3911.300 SARSTEDT AG & Co. KG, Nümbrecht, Germany) to continue the expansion. Once cIEC-H2 reached about 80% of confluency, they were frozen using a freezing medium composed of fetal bovine serum added with 10% of dimethyl sulfoxide (Cat.# 25-950-CQC- Corning Incorporated). From now, cells were routinely passed onto T-75 flasks with a seeding density of 5,500 cells/cm^2 using the expansion medium without puromycin. Cells used for the different assays were thawed at passage 4 and selected with puromycin for 7 d before being seeded on the required final supports. Every section about a specific assay reports the supports and the cell density used. If not specified, cells were seeded at 5,500 cells/cm^2.

During the different passages, the duplication time has been calculated as:

$$\left[\frac{\text{Days in culture}}{\frac{\ln\left(\frac{\text{number of seeded cells}}{\text{number of harvested cells}}\right)}{\ln(2)}}\right]$$

Lastly, to properly differentiate cIEC-H2 into mature enterocytes, a treatment with mouse epidermal growth factor (**mEGF**—Cat. # SRP3196—Sigma-Aldrich) was required. When cells were needed for challenges or assays, they were grown to full confluence, and then they were treated with 15 ng/mL of mEGF for 48 h before use. In Supplementary Figure 3, a prolonged transepithelial electrical resistance (**TEER**) measurement is reported to check the effects of long-term culture on TEER.

EdU Proliferation Assay and Growth Curve

To assess proliferative ability and the actual immortalization of cIEC-H2, 5-ethynyl-2′-deoxyuridine (**EdU**) incorporation, which can specifically mark the S-phase cells, was performed. The EdU-Click 488 (Cat.# BCK-EDU488- Sigma-Aldrich) was used. Briefly, freshly thawed cIEC-H2 passage 4 (thawed and selected with puromycin for 7 d before the assay) were seeded at a density of 2×10^4 cells/well onto Nunc Lab-Tek II Chamber Slide System (Cat.# 154534—Thermo Fisher Scientific, Waltham, MA) and after 48 h 10 μM EdU was added to the culture medium. After 4 h, cells were then fixed in 4% paraformaldehyde for 20 min at room temperature. After permeabilizing with 0.5% Triton X-100 in PBS for 20 min and rinsing 3 times with 3% bovine serum albumin (Cat.# P6154—VWR, Radnor, PA) in Dulbecco's phosphate-buffered saline (**DPBS**—Cat.# D8537—Sigma-Aldrich), cells were observed under the fluorescence upright microscope. The EdU-positive cells then showed up as a green color.

To characterize the growth of cIEC-H2 through the days and compare it with primary cIEC, a growth curve assay has been performed using the prestoblue cell viability reagent (Thermo Fisher Scientific). Briefly, cIEC-H2 (with a density of 1×10^4 cells/well) and primary cIEC (1200 aggregates/well) were seeded on 96-well plates with a working volume of 100 μL of complete medium. On d 0, 1, 2, 4, 7, 8, 9, 10, 11, 14, and 15, 10 μL of prestoblue were added to each well and after 1 h of incubation, the fluorescence (560 nm excitation and 590 nm emission) was read by varioskan LUX multimode microplate reader (Thermo Fisher Scientific).

Enzymatic Activity Assay

The presence of enzymatic activity was assessed on cIEC-H2 passage 40 (original cell line), cIEC-H2 passage 4 (thawed), and primary cIEC using alkaline phosphatase (**ALP**) fluorescence assay kit (Cat.# ab83369—Abcam plc., Cambridge, UK) following the manufacturer's instructions. cIEC-H2 (thawed and selected with puromycin for 7 d before the assay) and primary cells were seeded on 96-well plates (1×10^4 cells/well or 1,200 aggregates/well). Both were maintained at 37°C and 5% CO_2 until d 5. On d 5, cIEC-H2 were differentiated for 48 h with mEGF. On d 7, undifferentiated and differentiated cIEC-H2, and primary cells were used for the ALP assay kit.

Alkaline phosphatase cleaves the phosphate group of the nonfluorescent 4-methylumbelliferyl phosphate disodium salt (**MUP**) substrate resulting in an intense fluorescent signal that was read by varioskan LUX multimode microplate reader (330 nm excitation and

440 nm emission). The enzymatic activity was calculated as:

$$\text{ALP activity} = \frac{\frac{\text{nmol MUP generated}}{\text{volume of sample}}}{\text{reaction time}}$$

qPCR

Total RNA was isolated from freshly isolated primary cells (expanded for 7 d) or cells recovered from passaged cells or after the challenges using the nucleospin RNA kit (Cat. # 750955—Macherey-Nagel Inc., Allentown, PA), according to the manufacturer's protocol. RNA yield and quality were determined spectrophotometrically by detecting 260 and 280 nm absorbance by varioskan LUX multimode microplate reader (Thermo Fisher Scientific). Samples with a 260/280 ratio below 1.8 for DNA and 2.0 for RNA were excluded from the analyses. RNA was reverse transcribed with iScript cDNA synthesis kit (Cat. # 1708890—Bio-Rad Laboratories, Hercules, CA) according to the manufacturer's instructions. Lastly, real-time PCR reactions were performed in duplicate using CFX Connect Real-Time PCR System and iTaq Universal SYBR Green Supermix (Cat. # 1725120—Bio-Rad Laboratories).

Gene expression was reported as a fold of change using the ΔΔCt method (Livak and Schmittgen, 2001), using as reference the 60S acidic ribosomal protein P0 (***RPLP0***) and ribosomal protein L13 (***RPL13***). For the characterization of cIEC-H2 and the comparison with primary cIECs, specific markers were chosen, according to literature: E-cadherin (***CDH1***), villin (***VIL1***), cytokeratin 8 (***KRT8***), cytokeratin 18 (***KRT18***), cytokeratin 20 (***KRT20***), intestinal sucrase-isomaltase (***SUC-2***), maltase-glucoamylase (***MAGM***), intestinal alkaline phosphatase (***ALPi***), zonula occludens-1 (tight junction protein 1 —***ZO1***), occludin-1 (***OCLN***), claudin-1 (***CLDN1***), epithelial cell adhesion molecule (***EPCAM***), and vimentin (***VIM***). Markers typical of mesenchymal cells were also selected to exclude the mesenchymal nature of cIEC-H2: cluster of differentiation (**CD**)*45, CD90*, and *CD105*. To analyze the effects of the inflammatory and *Eimeria tenella* challenges, specific markers of innate immune response were chosen: interleukin (***IL***)*1B, IL6, IL8, IL10, IL17*, Toll-like receptor 4 (***TLR4***), and Interferon-gamma (***IFNG***). Lastly, to assess the expression changes of genes involved in the cell cycle caused by the immortalization, qPCR was performed specific markers: p53 tumor suppressor protein (***TP53***) cyclin-dependent kinase inhibitor 1 (also known as p21) (***CDKN1A***), retinoblastoma protein (also known as pRB) (***RB1***), cyclin-D1 (***CCND1***), cylin-E1 (***CCNE1***), and *c-MYC*.

All the primers (Sigma-Aldrich) were designed using the PrimerBLAST tool (https://www.ncbi.nlm.nih.gov/tools/primer-blast/) and they are listed in Table 2.

Immunofluorescence Assay

Immunofluorescence (**IF**) staining was performed for ZO1, OCLN, KRT18, and VIM, using the protocol already reported by Ghiselli et al. (2021a). Briefly, freshly thawed cIEC-H2 passage 4 (thawed and selected with puromycin for 7 d before the assay) were seeded at a density of 2×10^4 cells/well onto Nunc Lab-Tek II Chamber Slide System, cultured for 3 d until confluence and differentiated with mEGF for 48 h. Then they were fixed for 20 min with 4% paraformaldehyde (Cat.# 158127—Sigma-Aldrich) in DPBS. Cells were permeabilized with 0.5% Triton X-100 (Cat.# VARICP3418—VWR, Radnor, PA) for 15 min and then blocked in 10% goat serum (Cat.# G9023—Sigma-Aldrich) for 1 h. Primary monoclonal antibodies reported in Table 3 were diluted in 2% bovine serum albumin + 0.05% saponins (Cat.# A18820—Alfa Aesar, Haverhill, MA) in DPBS.

Cells were incubated with primary antibodies for 3 h at room temperature in a humidified chamber. Secondary antibodies conjugated to fluorescein isothiocyanate or tetramethylrhodamine were used to probe the bounded primary antibodies for 1 h (Table 2), followed by 2 successive washes with 0.2% bovine serum albumin + 0.05% saponins in DPBS. The slides were then mounted with fluoroshield containing 4′,6-diamidine-2′-phenylindole dihydrochloride (Cat.# F6057—Sigma-Aldrich). Images from 3 different fields were acquired with a Nikon Eclipse Ci fluorescence upright microscope with 20× or 40× magnification (Nikon corporation—www.nikon.com) and processed with NIS-Elements software (Nikon corporation).

Karyotype Determination

To address changes induced in the karyotype by immortalization and to confirm the chicken origin of these cells, a karyotype analysis has been performed. Freshly thawed cIEC-H2 passage 4 (thawed and selected with puromycin for 7 d before the assay) and primary cIEC were seeded on 24-well plates (5×10^4 cells/well; 7,200 aggregates/well—Cat.# 83.3922.300 SARSTEDT AG & Co. KG), and both were expanded at 37°C and 5% CO_2 for 48 h. On d 3, a medium change was performed, and after 1 h, 0.1 μg/mL of colcemid (Cat.# 10295892001- Sigma-Aldrich) was added to depolymerize microtubules and inactivate spindle fiber formation, thus synchronizing cells in metaphase. After 60 min with colcemid, cells were detached using Accutase and centrifuged at 125 *g* for 5 min. After the centrifuge, the supernatant was discarded and the pellet was resuspended in 37°C prewarmed 0.56% KCl solution and incubated for 25 min at 37°C. Then cells were centrifuged again at 125 *g* for 5 min. Supernatant was discarded and the pellet was resuspended in a cold solution of methanol:glacial acetic acid (3:1—fixative). The pellet was again centrifuged at 125 *g* for 5 min and resuspended again in fixative solution. A drop of resuspended chromosomes was released onto a microscope slide and allowed to

Table 2. Primer list used for gene expression.

	Gene	Primer sequence (5′→3′)	Product length (bp)	Accession N.
Epithelial markers	E-cadherin	F: TGAAGACAGCCAAGGGCCTG R: CTGGCGGTGGAGAGTGTGAT	109	NM_001039258
	Villin	F: GAACCTCTCGTGGCACCGC R: CTCATGTCCCTGCACCTCCC	152	XM_418521.5
	Cytokeratin 8	F: GTGTCCCAGTAGTTCCCCCAG R: CTGCTCCGCACAGATTTCCTG	131	XM_040654914.1
	Cytokeratin 18	F: CACAGATCCGGGAGAGCCTG R: CTCCACCGCGCTGTCATAGA	110	XM_025145666
	Cytokeratin 20	F: GCGCGTTATAAAGGAGGAGCTG R: CGCTGATTTACGGGCCGAAC	200	NM_204749.2
	EPCAM	F: GAACACGGCTGGTGTTAGGA R: CCACGTCGTCCTGACTAACT	76	NM_001012564.1
	Zonula occludens-1	F: TCTGCACAGTGAGGTTGGCT R: GGCTGTCCTGCATCGGTGT	145	XM_004934975
	Occludin-1	F: TGCTTTTGCCCAAGCAGGAA R: TGTGGGAGAGGCACCAGTTG	153	NM_204417
	Claudin-1	F: TCGGTGGTGGTCACTTCGTC R: CGCTGATTTACGGGCCGAAC	113	NM_001004768
	SUC-2	F: GGGAGCGAGATCAGTGGATG R: TTGTTCAGTGGGGCGTAGAC	120	XM_015275757.3
	MAGM	F: GCGAATTCTCCCCAAGTTGC R: CGGAGGTTGCAGAGGTTCTT	94	XM_040657177.1
	ALPi	F: AGTGTGCACCCATAGACAGC R: AGTCCATGCCCAGGATTTGG	76	XM_003641761.5
Cytokines	IL1B	F: TGCCTGCAGAAGAAGCCTCG R: CTCCGCAGCAGTTTGGTCAT	137	NM_204524.1
	IL6	F: GCAGGACGAGATGTGCAAGA R: ACCTTGGGCAGGTTGAGGTT	84	NM_204628.1
	IL8	F: AGCTGCTCTGTCGCAAGGTA R: GCTTGGCGTCAGCTTCACATC	124	NM_205498.1
	IL10	F: GTCACCGCTTCTTCACCTGC R: TCCCGTTCTCATCCATCTTCTCG	84	NM_001004414.2
	IL17	F: CAGCAAACGCTCACTGGCTC R: CTGGGCATCAGCAACCAAGC	82	NM_204460.1
	Interferon-γ	F: ACAACCTTCCTGATGGCGTG R: AGTTCATTCGCGGCTTTGCG	100	NM_205149.1
Other	Toll-like receptor 4	F: CCTGGGTCTAGCAGCCTTCC R: TGGCCCAGATTCAGCTCCTG	129	NM_001030693
	Vimentin	F: GCGCGATGTTCGTCAACAAT R: CGCAGGGCATCATTGTTCCT	123	NM_001048076.2
	CD45	F: TCCGACGCAGAGTGAATGCT R: AGCCCCTCCAACATAGCGTC	118	NM_204417.2
	CD90	F: GAACGTCTACCGGAACCGAG R: GTGTAGTCGTTGGTGGCCTT	126	NM_204381.2
	CD105	F: GCGAAAATAGCAACAGCCCC R: GTACAGCCCTTCACCTCACG	103	NM_001080887
Cell cycle	Cyclin-D1	F: CGAGGTGGAGACCATCCGAC R: GAAGTAGGACACCGAGGGCG	112	NM_205381
	Cyclin-E	F: CGTTCCTCCAGGATCCCGAC R: CCAGGACAGCTGGTTTTCGT	80	NM_001031358
	TP53	F: GCCGTGGCCGTCTATAAGAA R: GGTCTCGTCGTCGTGGTAAC	159	NM_205264.1
	CDKN1A	F: GAGAGCGACTGCGCTACAG R: GATCTGCTCGTGGTCTACGG	137	NM_001396336.1
	RB1	F: GGTGGCCGCTTGTACGG R: CATCGCACAGAGCCACGAAC	175	NM_204419.2
	c-MYC	F: CTGGTCCTCAAGCGGTGTCA R: GACCCTGCCACTGTCCAACT	114	XM_015283089
Ref.	RPLP0	F: TCACGGTAAAGAGGGGAGGTG R: CTTGCTCAGTCCCCAGCCTT	143	NM_205179
	RPL13	F: TCGTGCTGGCAGAGGATTC R: TCGTCCGAGCAAACCTTTTG	71	NM_204999

All primers were designed with PrimerBLAST.

Abbreviations: ALPi, intestinal alkaline phosphatase; CD, cluster of differentiation; CDKN1A, cyclin-dependent kinase inhibitor 1 (also known as p21); EPCAM, epithelial cellular adhesion molecule; MAGM, maltase-glucoamylase; RB1, retinoblastoma protein (also known as pRB); Ref., Reference genes; RPL13, ribosomal protein L13; RPLP0, ribosomal protein lateral stalk subunit P0; SUC-2, intestinal sucrase-isomaltase; TP53, p53 tumor suppressor protein.

air dry for 1 h. When dried, the slides were mounted with fluoroshield and observed under the microscope with 100× magnification in oil immersion. Twenty different complete spreads were analyzed and counted to determine the number of chromosomes. Karyotype analysis was performed using ImageJ imaging software (Schneider et al., 2012) with ChromosomeJ plugin (Uhlmann et al., 2016).

Table 3. Antibodies used for immunofluorescence assay.

Reagent	Dilution	Supplier	Product catalog number
Rabbit anti-chicken zonula occludens 1	10 μg/mL	Thermo Fisher Scientific	61-7300
Rabbit anti-chicken pan-occludin	2 μg/mL	Thermo Fisher Scientific	71-1500
Rabbit anti-villin	10 μg/mL	Abcam	ab130751
Mouse anti-chicken cytokeratin 18	10 μg/mL	Thermo Fisher Scientific	MA1-06326
Mouse anti-chicken vimentin	2 μg/mL	Thermo Fisher Scientific	MA5-11883
Goat anti-rabbit secondary antibody, FITC conjugated	4 μg/mL	Thermo Fisher Scientific	A27034
Donkey anti-mouse secondary antibody, TRITC conjugated	4 μg/mL	Thermo Fisher Scientific	A27034

Abbreviations: FITC, fluorescein isothiocyanate; TRITC, tetramethylrhodamine.

Inflammatory Challenge

Freshly thawed cIEC-H2 passage 4 (thawed and selected with puromycin for 7 d before the assay) were seeded at a density of 5×10^4 cell/filter onto 24 well Transwell polyethylene terephthalate inserts (0.4 μm pore—Cat.# 3413 Corning Incorporated) and were maintained at 37°C and 5% CO_2 until d 5. On d 5, confluent cells were differentiated for 48 h with mEGF and on d 7 were monitored by measuring TEER. On d 7, inflammatory challenge was induced for 6 h and consisted of the exposure to *Escherichia coli O55:B5* lipopolysaccharide (**LPS**—Cat.# L2880—Sigma-Aldrich) and a cocktail of chicken pro-inflammatory cytokines (adapted from Van De Walle et al., 2010). In the apical compartment, only LPS 1 μg/mL or 30 μg/mL was used. On the basolateral side, cells were challenged using LPS 1 μg/mL or 30 μg/mL in combination with chicken pro-inflammatory cytokines: IL1B 25 ng/mL (Cat.# abx670113—Abbexa Ltd., Cambridge, UK), Tumor-necrosis factor alpha (**TNF**) 50 ng/mL (Cat.# abx166366—Abbexa Ltd.), and IFNG 50 ng/mL (Cat. # RP0115C—Kingfisher Biotech Inc., St. Paul, MN). To determine the monolayer integrity, TEER was measured before the challenge and after 2 h, 4 h, and 6 h. In the end, cells were harvested to perform qPCR analyses. TEER was measured with a volt-ohm meter (Millicell ERS-2, Cat. # MERS00002—Millipore, Burlington, MA), then values were calculated as: $[(cell\ well\ TEER -- blank\ well\ TEER) \times well\ area\ size\ (\Omega \cdot cm2)]$.

Eimeria Invasion Assay

Freshly thawed cIEC-H2 passage 4 (thawed and selected with puromycin for 7 d before the assay) were seeded on 24-well plates at a density of 5×10^4 cells/well and were maintained at 37°C and 5% CO_2 until d 5. On d 5, confluent cells were differentiated for 48 h with mEGF.

After differentiation, the cells were infested with *E. tenella* sporozoites and purified as follows. The oocysts stored in 2% potassium dichromate (Cat.# P5271, Sigma-Aldrich) were washed and resuspended in 10% sodium hypochlorite for sterilization, then they were washed and lysed with glass beads (1 mm) for 2 min at 33 Hz with TissueLyser (Cat.# 85600, Qiagen, Hilden, Germany) to obtain sporocysts. Those were washed and resuspended in an excystation medium, containing 2.5 g/L trypsin (Cat.# P10-025025P, Pan-Biotech GmbH, Aidenbach, Germany), 5 g/L bile salts (Cat.# B3301, Sigma-Aldrich), and 2 g/L $MgCl_2$ (Cat.# 459337, Carlo Erba Reagents, Milan, Italy). The suspension was incubated for 90 min at 41°C in a heating block (Cat# HM100-Pro, DLAB Scientific Co., Beijing, China). Afterward, the obtained sporozoites were purified with PluriStrainer 5 μm (Cat# 43-50005-13, pluriSelect Life Science, Leipzig, Germany), washed, and resuspended in mEGF supplemented-cell medium at a concentration of 1×10^5 intact sporozoites/well, to initiate the invasion assay. Sporozoites' membrane integrity was visually checked using a trypan blue exclusion test diluting 10 μL of sporozoites suspension with 10 μL of trypan blue solution (Cat.# T8154-, Sigma-Aldrich) and counting with a Burker chamber the intact ones.

The invasion assay was performed for 4 h and 24 h. Afterward, the cell supernatant was collected to count extracellular sporozoites, to assess invasion efficiency with the following formula:

$$100 - \left[\left(\frac{\text{number of sporozoites in the supernatant after treatment}}{\text{number of starting sporozoites}}\right) \times 100\right]$$

The cells were washed, at both time points, twice with DPBS and then they were lysed to perform nucleic acids (DNA and RNA) extraction, with the NucleoSpin TriPrep Kit (Cat. # 740966—Macherey-Nagel Inc.), as described by the manufacturer's instructions.

Eimeria *Quantification by Standard Absolute PCR Quantification*

The amplification target was cloned on a pUC57-mini plasmid (GenScript Biotech Corp, Piscataway, NJ) carrying the sequence of *E. tenella* internal transcribed spacer-1 (**ITS-1**). The primers reported in Table 4 were used to generate the 147 bp sequence. The *ITS-1* gene is a conserved region commonly employed for species identification and it is expressed by sporozoites and other developmental stages (Kawahara et al., 2008). qPCR was performed as described in the previous section. Ten-fold serial dilutions of the cloned plasmid were amplified and used to generate a standard quantification curve. The unknown samples were amplified and then the *ITS-1* copies were quantified by interpolation.

Table 4. *Eimeria tenella* amplicon sequence and primers used for the absolute quantification.

Gene	Amplicon sequence (5′→3′)			
	TGGAGGGGATTATGAGAGGAGAAGACGCGCACGGGGCTGTGTCGTATGCAGAGCGCTCGCGGCTCGGGCGA TTGTTCCGTGTTGTGTGCTCTGCTGCATGCTGGTGTGTGCGTTCTGTCTCTTTCTCTCTCCGTTACATGCTGCTTG			
E. tenella ITS-1	Primer sequence (5′→3′)	Product length (bp)	Accession N.	Reference
	F: TGGAGGGGATTATGAGAGGA R: CAAGCAGCATGTAACGGAGA	147	AF026388	(Kawahara et al., 2008)

Abbreviation: ITS-1, internal transcribed spacer -1.

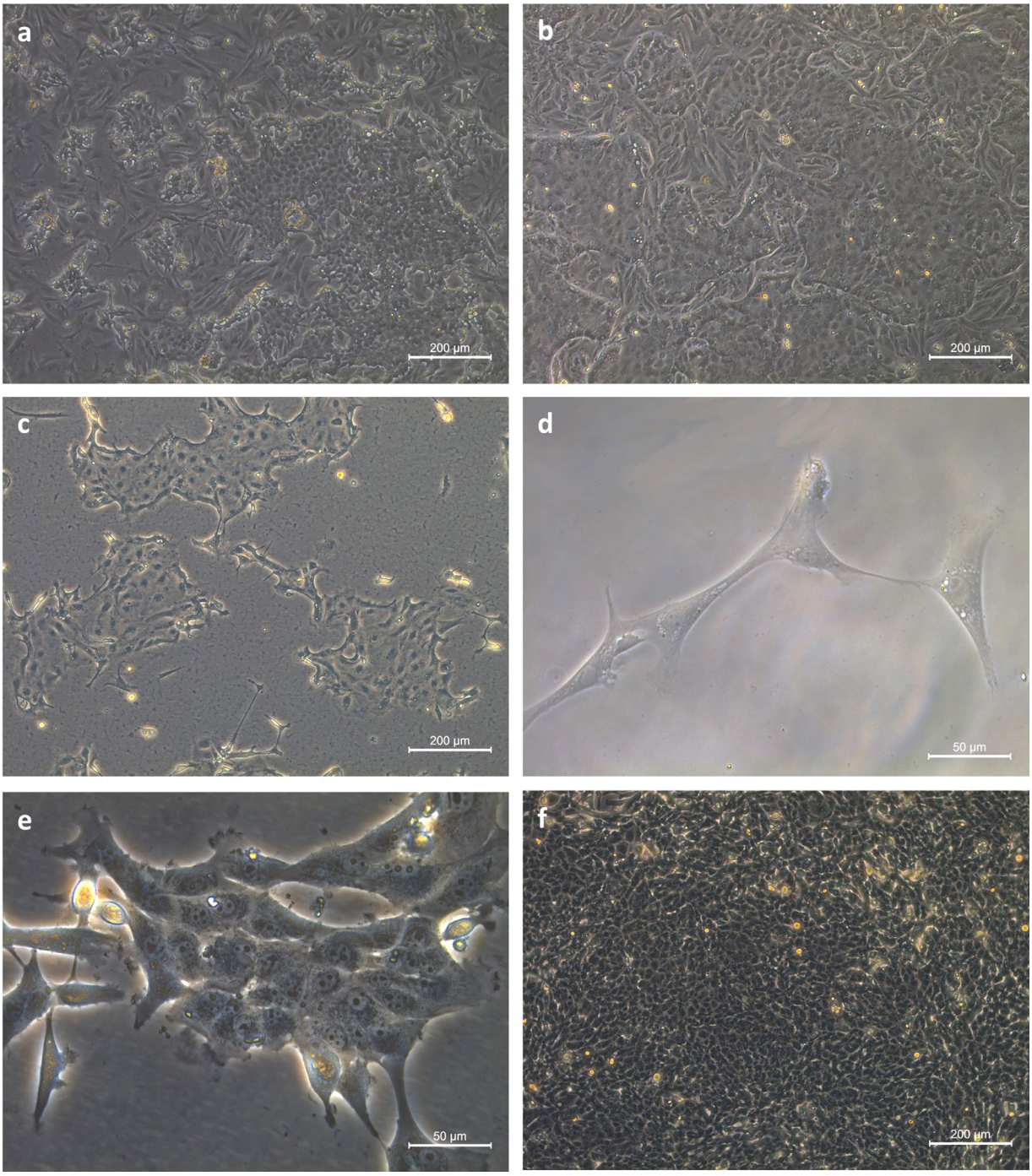

Figure 1. Establishment of cIEC-H2. (a) Primary cIEC on Matrigel-coated wells before lentiviral transfection; (b) primary cIEC on Matrigel-coated wells after 24 h of incubation with the lentiviral vector; (c) primary cIEC on Matrigel-coated wells 2 d after lentiviral transfection; (d) cells 24 h after a single cell were seeded through limiting dilution method; (e) cells 72 h after limiting dilution monoclonal selection; (f) confluent transformed cIEC after 15 d of puromycin (4 ppm) selection. All the pictures were taken with a 10× magnification except for figure d) and e) that were captured with a 40× magnification in 3 different fields.

Statistics and Reproducibility

The legends of each figure provide more details about sample sizes, numbers of replicates, and statistics used. All data were represented as mean ± standard error (**SEM**). Statistical analysis was performed using Graph-pad Prism 9.5 (https://www.graphpad.com/scientific-software/prism/). Shapiro−Wilk's test was used to assess the normal distribution, samples with $P > 0.05$ were accepted as normally distributed. Outliers were defined by the ROUT Method with the False Discovery Rate (Q) set >1% and excluded from the analysis. All measurements were recorded from distinct samples. Samples involved in qPCR with a 260/280 ratio below 1.8 for DNA and 2.0 for RNA were excluded from the analyses.

TEER readings ($n = 6$) and gene expression data after *E. tenella* invasion data ($n = 6$) were normally distributed and analyzed using 2-way ANOVA and mixed-model analysis respectively with Šídák's multiple comparisons test with time and treatment as factors. qPCR on cell characterization data ($n = 5$), cell-cycle genes expression data ($n = 4$), LPS inflammatory challenge data ($n = 6$), and ALP activity ($n = 5$) were normally distributed and analyzed using 1-way ANOVA with Tukey's multiple comparisons.

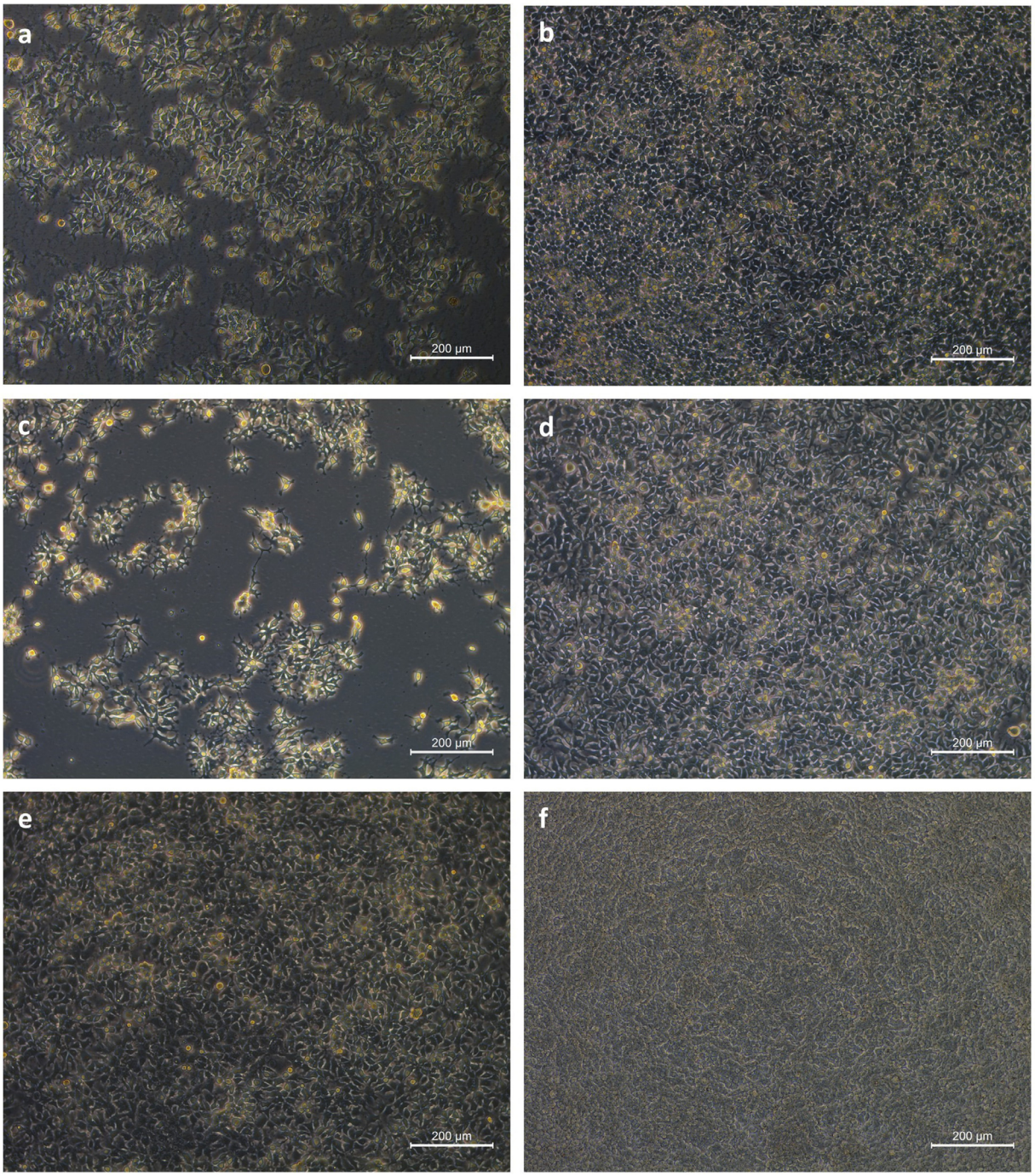

Figure 2. cIEC-H2 growth over time. (a) Low confluency cIEC-H2 P3; (b) full confluent cIEC-H2 P3; (c) low confluency cIEC-H2 P5, 3 passage post-thaw; (d) full confluent cIEC-H2 P5, 3 passage post-thaw; (e) full confluent cIEC-H2 P30 before mEGF differentiation; (f) full confluent cIEC-H2 P30 after 48 h of mEGF differentiation. All the pictures were taken with a 10× magnification.

E. tenella internalization data ($n = 8$) were normally distributed and analyzed using an unpaired 2-tailed t test. The level of significance (p) was set at 0.05 for all the analyses.

RESULTS

Cell Immortalization

Intestinal cell aggregates rapidly attached to the Matrigel-coated wells and cells gradually migrated out from the foci of proliferation within 24 h in culture, as is visible in Figure 1a. Cells were then incubated for 24 h with the lentiviral vector and reached confluency (Figure 1b). Two days after the transduction, cells appeared with a cobblestone morphology organized in little islands (Figure 1c). Using the limiting dilution method, cells were seeded one per well and after 24 h, they started to proliferate (Figures 1d and 1e). Then the puromycin selection started and after 15 d transformed cIEC resulted in a fully confluent monolayer of cells with a cobblestone morphology (Figure 1f).

Culture Conditions and Differentiation

After limiting dilution and puromycin selection cIEC-H2 were propagated in different support to amplify the population. In Figure 2, low confluency (Figure 2a) and full confluent (Figure 2b) cIEC-H2 P3 are reported. Cells maintained a stable morphology and growth characteristics during several passages and also after the freeze/thawing cycle. Figures 2c and 2d report thawed cIEC-H2 after 3 passages (P5). After differentiation, cells appeared more compact and tightened together, as reported in Figure 2, where full confluent cIEC-H2 P30 before (Figure 2e) and after (Figure 2f) mEGF differentiation are represented. During different passages, cells maintained also a constant duplication time. Figure 3 reports the duplication times of the original cIEC-H2 through all the passages from the isolation of primary cells to cIEC-H2 P40 and of thawed cIEC-H2 from P2 to P9.

EdU Proliferation Assay and Growth Curve

To assess the proliferative capability and the growth curve an EdU assay and a Prestoblue growth curve were performed. From the EdU assay reported in Figure 4a, it is possible to see numerous S-phase cells confirming the proliferative capability of those cells. Figure 4b reports the graph obtained from the proliferative growth curve performed both on primary cells and immortalized cells, showing a very quick expansion through the days. Moreover, immortalized cells maintain higher viability levels without the degeneration that occurs between d 11 and 14 with primary cells.

qPCR Characterization

cIEC-H2 showed the presence of all different epithelial markers in qPCR also when undifferentiated as reported

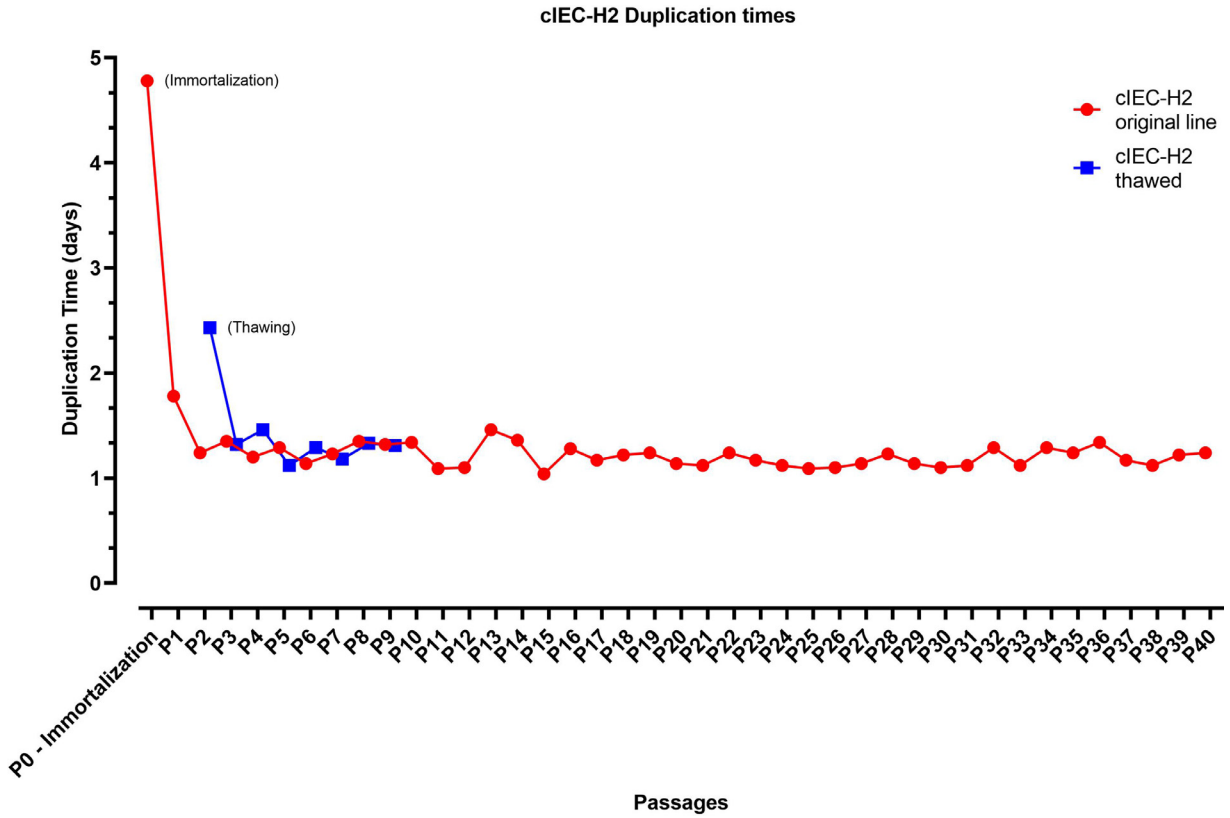

Figure 3. Duplication time (d) of the original cIEC-H2 (red line) through all the passages from the immortalization to P40 and of thawed cIEC-H2 (blue line) from P2 to P9.

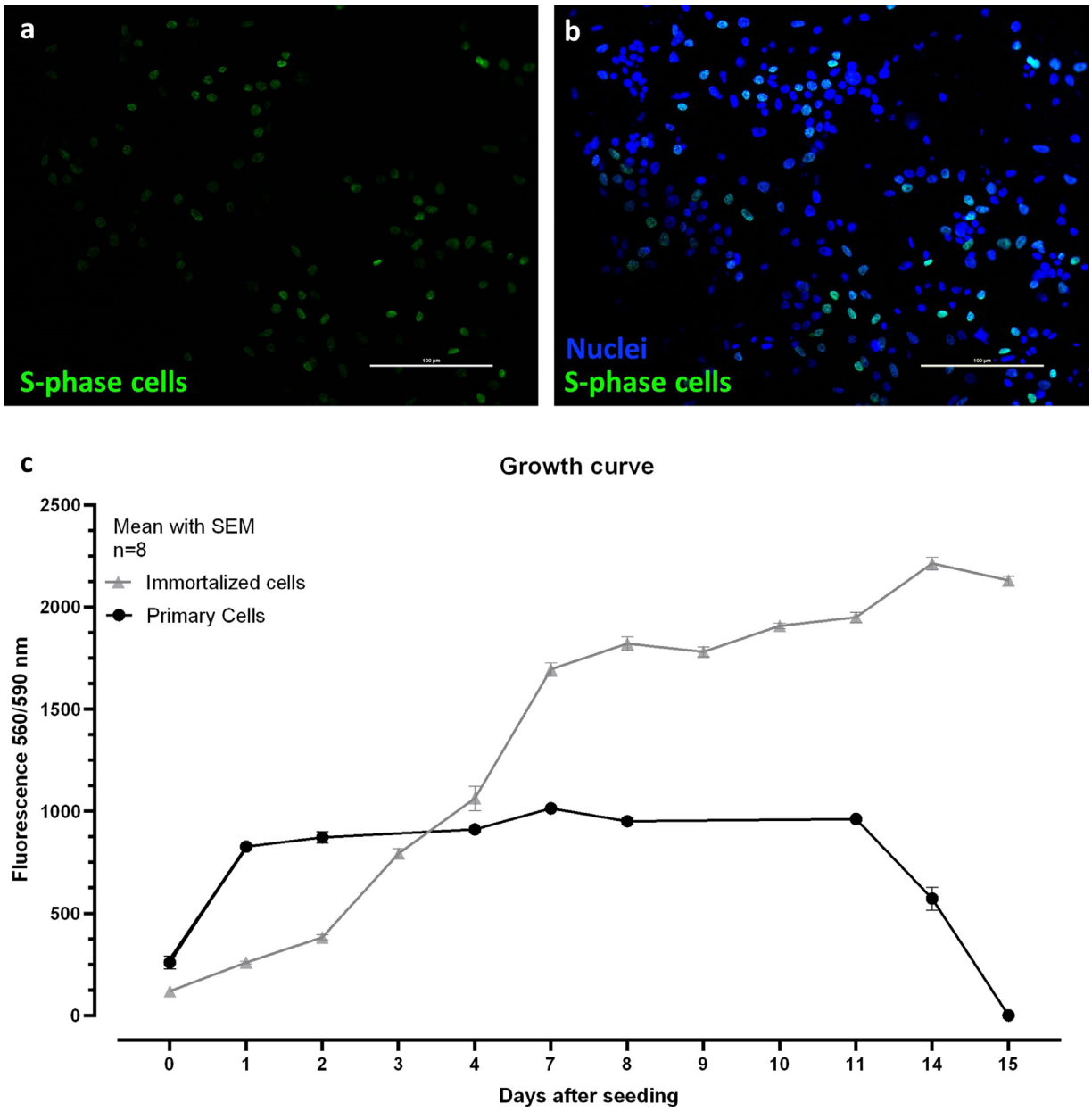

Figure 4. cIEC-H2 passage 4 growth characterization. (a) EdU staining at 2 d after seeding FITC only (b) EdU staining at 2 d after seeding FITC+DAPI. Pictures were taken with a 20× magnification in 3 different fields; (c) PrestoBlue reagent viability reported as fluorescence units (excitation 560 nm; emission 590 nm) from d 0 after seeding to d 15 for primary cIECs (black dots and black line) and cIEC-H2 (gray triangles and gray line). Data are represented as mean with SEM ($n = 8$).

in Figure 5. The differentiation for 48 h with mEGF significantly increased the expression of *CDH1* ($P < 0.0001$), *KRT20* ($P = 0.0008$), *OCLN* ($P < 0.0001$), *CLDN1* ($P < 0.0001$), *EPCAM* ($P < 0.0001$), and *VIM* ($P < 0.0001$). Moreover, the expression of *VIL1, ZO1,* and *KRT8* was unchanged and *KRT18* had a significant ($P < 0.0001$) decrease. Comparing the mRNA expression of the same markers with primary cells it is possible to notice that differentiated cIEC-H2 showed higher *CDH1* ($P < 0.0001$), *EPCAM* ($P < 0.0001$), *KRT20* ($P = 0.0048$), *OCLN* ($P = 0.0008$), *CLDN1* ($P < 0.0001$), and *ALPi* ($P = 0.0026$). On the other hand, differentiated cIEC-H2 had lower *ZO1* ($P = 0.0073$) and *KRT18* ($P < 0.0001$); *VIL1, KRT8, SUC-2*, and *MAGM* have similar mRNA expression levels. Lastly, *CD45, CD90*, and *CD105* expression was not detected both in primary and immortalized cells. Supplementary Figure 4 reports a transcript levels comparison of selected markers between never cryopreserved (passage 15) and cryopreserved (passage 4) cIEC-H2.

Immunofluorescence Characterization

Confluent cells were stained after mEGF differentiation for phenotype characterization. Differentiated cIEC-H2 were positive for ZO1, OCLN, KRT18, and VIL1 (Figure 6), thus confirming the epithelial nature of these cells, as shown in Figure 6. Immunofluorescence showed also low VIM positivity in undifferentiated cells, which was not observed in the differentiated ones.

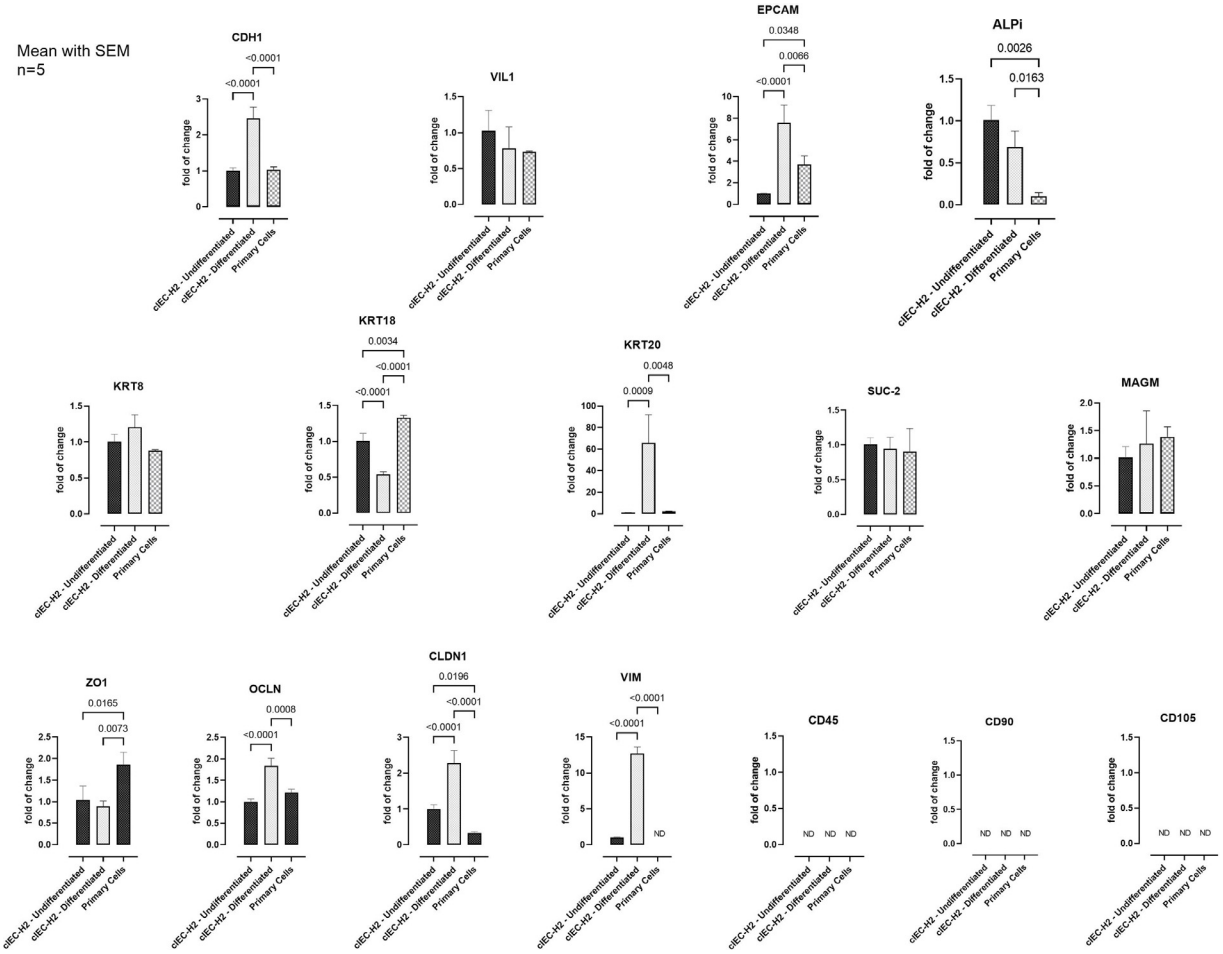

Figure 5. qPCR characterization of primary cIECs and cIEC-H2 passage 4 pre- and post-mEGF differentiation. Data are reported as fold change calculated using the ΔΔCT method. RNA samples with a 260/280 ratio below 2.0 were excluded from the analysis. Outliers were defined by the ROUT Method with the False Discovery Rate (Q) set >1% and excluded from the analysis. Data were normally distributed (Shapiro−Wilk test $P > 0.05$) and analyzed using one-way ANOVA with Tukey's multiple comparisons. CDH1: undifferentiated vs. differentiated $P < 0.0001$, 95% CI −1.848 to −1.074, differentiated vs. primary $P < 0.0001$, 95% CI 0.9348−1.933—EPCAM undifferentiated vs. differentiated $P < 0.0001$, 95% CI −8.590 to −4.591, undifferentiated vs. primary $P = 0.0348$, 95% CI −5.204 to −0.2155, differentiated vs. primary $P = 0.0066$, 95% CI 1,299 −6,462—VIM: undifferentiated vs. differentiated $P < 0.0001$, 95% CI −12.90 to −10.54, differentiated vs. primary $P < 0.0001$, 95% CI 10.68−14.76 —KRT18 undifferentiated vs. differentiated $P < 0.0001$, 95% CI 0.3084−0.6180, undifferentiated vs. primary $P = 0.0034$, 95% CI −0.5174 to −0.1313, differentiated vs. primary $P = 0.0066$, 95% CI −0.9874 to −0.5877—KRT20: undifferentiated vs. differentiated $P = 0.0009$, 95% CI −95.54 to −33.69, differentiated vs. primary $P = 0.0048$, 95% CI 23.35 to 103.2− ALPi: undifferentiated vs. primary $P = 0.0026$, 95% CI 0.4351 −1.381, differentiated vs. primary $P = 0.0163$, 95% CI 0.1393−1.036—ZO1: undifferentiated vs. primary $P = 0.0165$, 95% CI −1.467 to −0.1825, differentiated vs. primary $P = 0.0073$, 95% CI −1,612 to −0.3270—OCLN: undifferentiated vs. differentiated $P < 0.0001$, 95% CI −1.066 to −0.6087, differentiated vs. primary $P = 0.0008$, 95% CI 0.3244 to 0.9145—CLDN1: undifferentiated vs. differentiated $P < 0.0001$, 95% CI −1.718 to −0.8292, undifferentiated vs. primary $P = 0.0196$, 95% CI 0.1251−1.234, differentiated vs. primary $P < 0.0001$, 95% CI 1.379−2.527. Data are represented as mean with SEM ($n = 5$). Abbreviations: ALPi = intestinal alkaline phosphatase; CDH1 = E-cadherin; CLDN1 = claudin 1; EPCAM = epithelial cellular adhesion molecule; KRT18 = cytokeratin 18; KRT20 = cytokeratin 20; KRT8 = cytokeratin 8; MAGM = maltase-glucoamylase; OCLN = occludin; SUC-2 = intestinal sucrase-isomaltase; VIL1 = villin; VIM =vimentin; ZO1= zonula occludens 1.

Karyotype Determination and Cell-Cycle

In Figures 7a and 7b, the karyotype of cIEC-H2 and primary cIEC is respectively reported. Chromosomes number were counted on 20 different spreads and no aberrations on chromosome number have been observed. cIEC-H2 showed a normal chicken diploid karyotype with 39 pair of chromosomes. Macro- and microdistribution of chromosome is conserved with no visible numeric alterations. In Figure 7e, the gene expression analysis of some important cell-cycle genes is reported. Comparing undifferentiated cIEC-H2 and primary cIEC *RB1* ($P = 0.0136$), *TP53* ($P < 0.0001$), *CDKN1A* ($P < 0.0001$), *CCND1* ($P = 0.014$), and *CCNE1* ($P < 0.0001$) were significantly downregulated on immortalized cells and *c-MYC* mRNA expression was significantly ($P = 0.0026$) upregulated in cIEC-H2. Lastly, the mEGF differentiation showed a significant downregulation of *CDKN1A* ($P = 0.0121$) and *CCNE1* ($P = 0.0129$). The other tested genes were not significantly affected by mEGF differentiation.

Enzymatic Activity Assay

Figure 8 represents the results of the ALP activity assay. cIEC-H2 maintained ALP enzymatic activity around 50 mU/L similarly to the freshly isolated

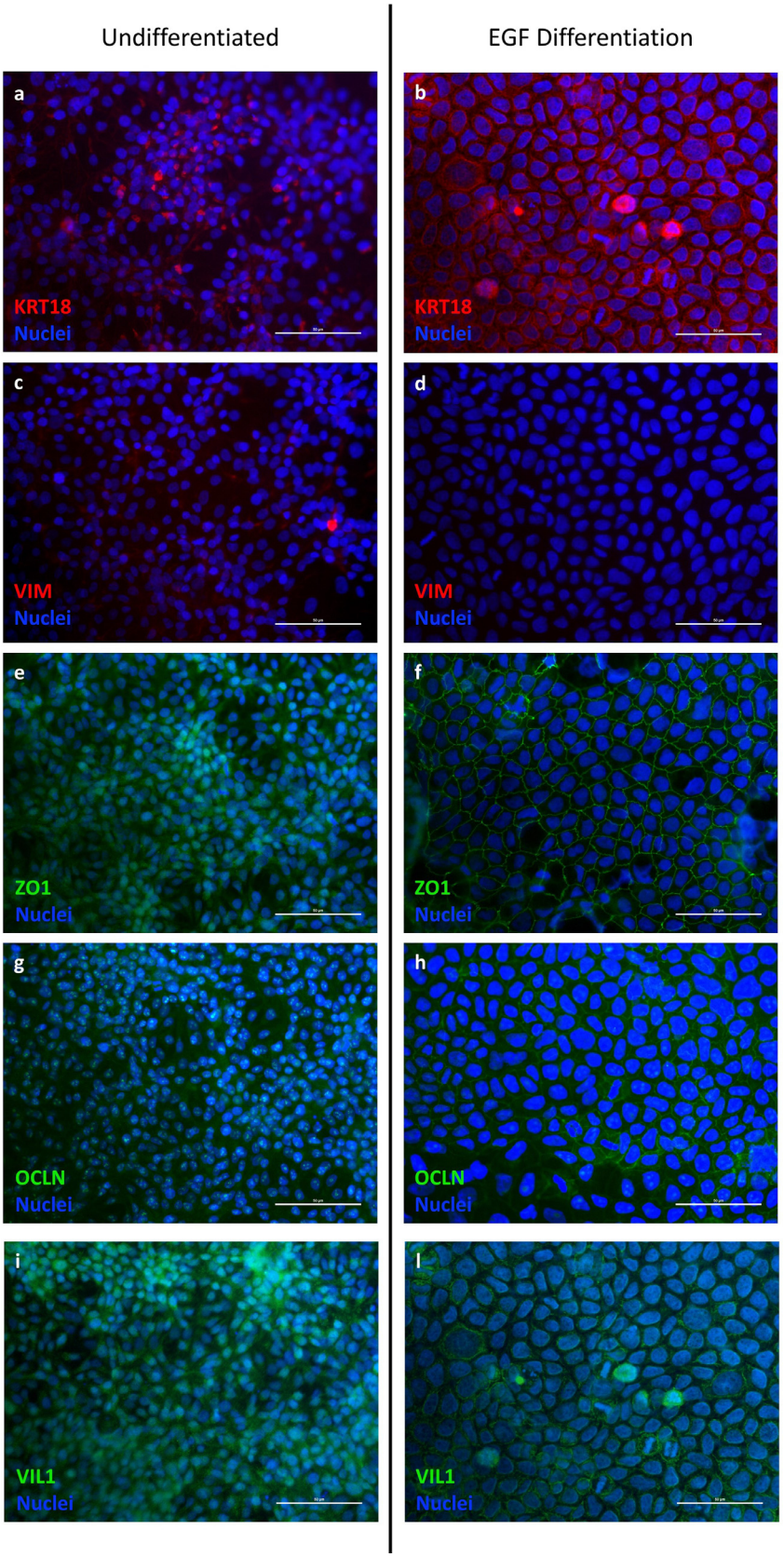

Figure 6. IF characterization of cIEC-H2 passage 4 pre (a; c; e; g; i) and post (b; d; f; h; l) mEGF differentiation. (a) KRT18 (red) in undifferentiated cells; (b) KRT18 (red) in differentiated cells; (c) VIM (red) in undifferentiated cells; (d) VIM (red) in differentiated cells; (e) ZO1 (green) in undifferentiated cells; (f) ZO1 (green) in differentiated cells; (g) OCLN (green) in undifferentiated cells; (h) OCLN (green) in differentiated cells; (i) VIL1 (green) in undifferentiated cells; l) VIL1 (green) in differentiated cells. Pictures were taken with a 40x magnification in three different fields. Abbreviations: KRT18, cytokeratin 18; OCLN, occludin; VIM, vimentin; VIL1, villin; ZO1, Zonula occludens 1.

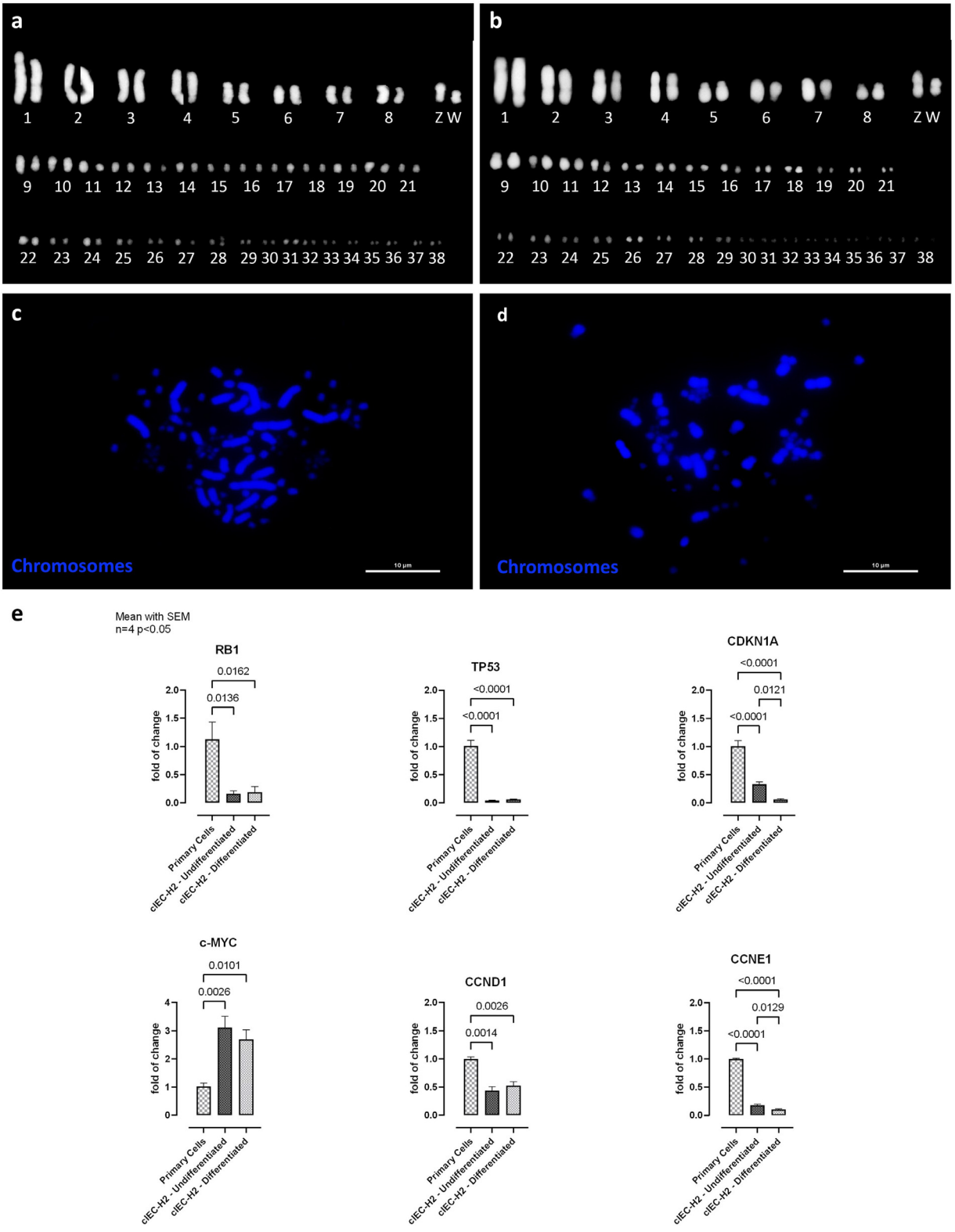

Figure 7. Karyotype and cell-cycle genes mRNA expression. (a) cIEC-H2 karyotype; (b) primary cIEC karyotype; (c) cIEC-H2 chromosomes spread; (d) primary cIEC chromosomes spread. Pictures were taken with at 100× magnification in oil immersion. Twenty different spreads were analyzed. (e) Effect of immortalization on cell-cycle genes in qPCR expression. Data are reported as fold change calculated using the ΔΔCT method. RNA samples with a 260/280 ratio below 2.0 were excluded from the analysis. Outliers were defined by the ROUT Method with the False Discovery Rate (Q) set >1% and excluded from the analysis. Data were normally distributed (Shapiro−Wilk test p>0.05) and they were analyzed using a one-way ANOVA with Tukey's multiple comparisons. RB1: undifferentiated vs. primary $P = 0.0136$, 95% CI 0.2251−1.716, differentiated vs. primary $P = 0.0162$, 95% 0.1943−1.6851—TP53: undifferentiated vs. primary $P < 0.0001$, 95% CI 0.7384−1.199, differentiated vs. primary $P < 0.0001$, 95% 0.7244−1.185—CDKN1A: undifferentiated vs. primary $P < 0.0001$, 95% CI 0.4597 to 0.8931, differentiated vs. primary $P < 0.0001$, 95% 0.7299−1.163, undifferentiated vs. differentiated $P = 0.0121$, 95% CI 0.06960−0.4709—c-MYC: undifferentiated vs. primary $P = 0.0026$, 95% CI −3.313 to −0.8724, differentiated vs. primary $P = 0.0101$, 95% −2.894 to −0.4534—CCND1: undifferentiated vs. primary $P = 0.0014$, 95% CI 0.2847−0.8447, differentiated vs. primary $P = 0.0026$, 95% 0.2146−0.7384—CCNE1: undifferentiated vs. primary $P < 0.0001$, 95% CI 0.7621−0.8809, differentiated vs. primary $P < 0.0001$, 95% 0.8401−0.9589, undifferentiated vs. differentiated $P = 0.0129$, 95% CI 0.01861−0.1374. Data are represented as mean with SEM ($n = 4$). Abbreviations: CCND1, cyclin-D1; CCNE1, cyclin-E1; CDKN1A, cyclin-dependent kinase inhibitor 1 (also known as p21); RB1, retinoblastoma protein (also known as pRB); TP53, p53 tumor suppressor protein.

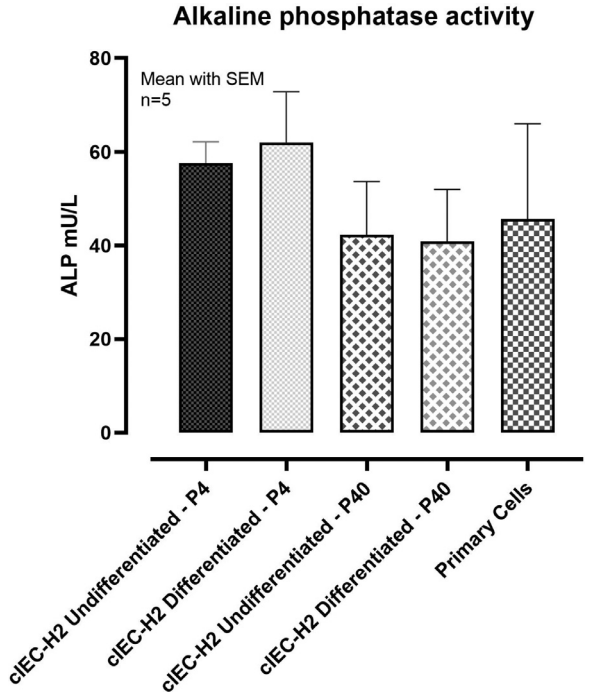

Figure 8. Alkaline phosphatase activity (mU/L) of primary cIEC and cIEC-H2 pre- and post-mEGF differentiation. P4 = thawed cells; P40 = original cell line never cryopreserved. Unit = The amount of enzyme causing the hydrolysis of 1 μmole of 4-methylumbelliferyl phosphate disodium salt per minute at pH 10.0 and 25°C. Data are represented as mean with SEM ($n = 5$). Outliers were defined by the ROUT Method with the False Discovery Rate (Q) set >1% and excluded from the analysis. Data were normally distributed (Shapiro–Wilk test $P > 0.05$) and analyzed using a one-way ANOVA with Tukey's multiple comparisons. No significant differences were detected.

primary cells until passage 40 and also after thawing. mEGF differentiation and cryopreservation did not affect ALP activity. Primary cells recorded an ALP activity value of 45.68 ± 20.29 mU/L. cIEC-H2 at passage 40 (never cryopreserved) showed an activity value of 42.24 ± 19.78 mU/L before mEGF treatment and 40.86 ± 19.27 mU/L after differentiation. Lastly, cIEC-H2 passage 4 (after cryopreservation) recorded and ALP activity value of 57.59 ± 4.53 mU/L before differentiation and 61.96 ± 10.90 mU/L after differentiation.

Inflammatory Challenge

Figure 9a reports the TEER values measured at 2 h, 4 h, and 6 h after the challenge. Both LPS used at 1 μg/mL or 30 μg/mL in combination with cytokines significantly reduced the TEER values by (20.919 ± 1.029) % 4 h for LPS 1 μg/mL and (26.689 ± 3.720) % 4 h for LPS 30 μg/mL after the start (LPS 1 μg/mL: $P = 0.0015$; LPS 30 μg/mL: $P < 0.0001$) compared to the initial TEER. These differences remained then stable after 6 h. Moreover, the effects of inflammatory challenge, reported in Figure 9b, are also visible on qPCR gene expression. LPS used at 1 μg/mL in combination with cytokines significantly increased *IL6* ($P = 0.0468$), and *IL1B* ($P = 0.0173$) but no effect was observed on other tested markers. LPS used at 30 μg/mL in combination with cytokines significantly increased *IL6* ($P = 0.0282$), and *IL1B* ($P = 0.0454$) and decreased *IL10* ($P = 0.0027$) and *TLR4* ($P = 0.0133$) levels, confirming the ability of this immortalized cell line to produce an innate immune response when exposed to pro-inflammatory conditions.

Eimeria *Invasion Assay*

Figure 10 reports the invasion efficiency of *E. tenella* sporozoites at 4 and 24 h postinvasion (**HPI**) assessed with supernatant counts (Figure 10a) and *ITS-1* standard DNA quantification (Figure 10b). This cell model was found to be susceptible to *E. tenella* sporozoites invasion, as demonstrated by the progressive increase in the invasion efficiency; significant differences were found between 4 and 24 HPI by both methods (supernatant counts $P < 0.0001$; standard DNA quantification $P = 0.0114$). Counting the sporozoites in the supernatant the invasion efficiency increased from (66.23±1.48) % 4 HPI to (89.40±1.84) % 24 HPI. Moreover, the qPCR detected (33,993 ± 1,087) *ITS-1* copies 4 HPI and (50,211 ± 5,010) 24 HPI showing an increase of about 32% between the 2 time points.

Lastly, the *E. tenella* invasion induced a significant increase in the cytokines typical of the innate immune response, confirming the ability of this model to respond to coccidia infection, as reported in Figure 10c. After 24 HPI *IL6* ($P = 0.113$), *IL1B* ($P = 0.0014$), *IL10* ($P = 0.0262$), and *IFNG* ($P = 0.0472$) were upregulated by 2-folds and *IL8* ($P < 0.0001$) by near 5-folds. *IL17* was not affected by the *E. tenella* invasion.

DISCUSSION

At the time of publication, no immortalized chicken intestinal epithelial cell line had ever been established, fully characterized, and published. There are 2 commercially available avian intestinal cell lines, an SV40-immortalized line (Accegen) and a clonal line (CHIC-8E11) but detailed scientific studies regarding their in-depth characterization, required for validating its suitability as a research model, are currently lacking.

In this study, a novel immortalized avian intestinal epithelial cell line was developed, starting from 19-day-old chicken embryos. The cIEC-H2 cell line showed to be stable up to 40 doublings, and it can be frozen and thawed successfully without any alteration. Moreover, when the cells reach the full confluence, after 48 h of differentiation with mEGF, cIEC-H2 express all the typical markers of mature enterocytes and they maintain proper enzymatic activity and innate immune response capabilities against pathogen-associated molecular patterns. We showed that this cell line is susceptible to the invasion of *E. tenella* sporozoites, as well as other models of nonintestinal origins, commonly used to perform invasion studies (Felici et al., 2021). This model was successfully used to study the primary host response, providing some valuable insights on the host–pathogen interactions during invasion. Also, due to the longer time in

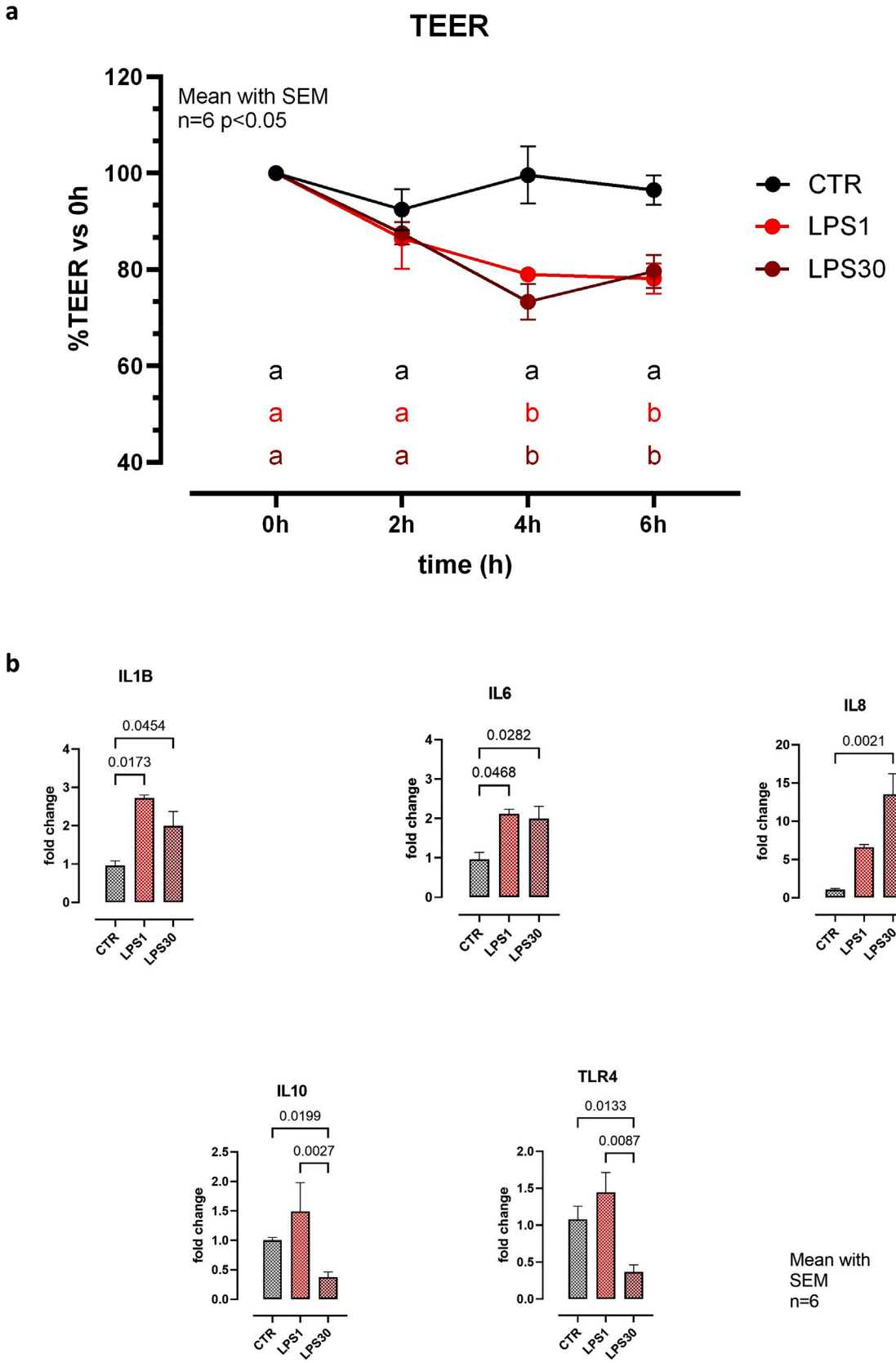

Figure 9. Effect of inflammatory challenge on cIEC-H2 passage 4. CTR = Unchallenged control group; LPS1 = In the apical compartment, LPS from *Escherichia coli* O55:B5 at 1 μg/mL. In the basolateral side, LPS 1 μg/mL + IL1B 25 ng/mL + TNF 50 ng/mL + IFNG 50 ng/mL; LPS30 = In the apical compartment LPS from *E. coli* O55:B5 at 30 μg/mL. In the basolateral side, LPS 30 μg/mL + IL1B 25 ng/mL + TNF 50 ng/mL + IFNG 50 ng/mL. (a) Transepithelial electrical resistance (TEER) values were recorded after 0 h, 2 h, 4 h, and 6 h after the challenge. Outliers were defined by the ROUT Method with the False Discovery Rate (Q) set >1% and excluded from the analysis. Data were normally distributed (Shapiro−Wilk test $P > 0.05$) and analyzed using 2-way ANOVA ($P < 0.05$) with Šídák's multiple comparisons tests. 4 h: *CTR* vs. *LPS1* $P = 0.0015$, 95% CI 5.682−35.53, *CTR* vs. *LPS30* $P < 0.0001$, 95% CI 12.07−40.53—6 h: *CTR* vs. *LPS1* $P = 0.0064$, 95% CI 3.493−33.34, *CTR* vs. *LPS30* $P = 0.0097$, 95% CI 2.682−31.14. Data are represented as mean with SEM ($n = 6$). (b) Effect of challenge on innate immune response makers

culture, we believe that this model could represent a valid tool for further research on the *Eimeria* development in vitro.

In literature, different protocols to culture primary chicken enterocytes or organoids are present (Dimier-Poisson et al., 2004; Immerseel et al., 2004; Pierzchalska et al., 2012; Guo et al., 2015; Yuan et al., 2015; Kaiser et al., 2017; Bar Shira and Friedman, 2018; Li et al., 2018; Rath et al., 2018; Nash et al., 2021; Orr et al., 2021; Ghiselli et al., 2021a; Oost et al., 2022). Previously, our research group published a method to culture primary cIEC starting from 19-day-old chicken embryos (Ghiselli et al., 2021a). These cells survive for 10 to 12 d in culture and they express the typical enterocyte markers; also, a TEER value was measured for the first time (Ghiselli et al., 2021a). This was a promising model but those cells could survive only for a short period in culture. Moreover, they require pretty expensive coatings and media to be cultured. These drawbacks are also common in 3D basal-out avian organoids models (Pierzchalska et al., 2012; Oost et al., 2022). Nash et al. (2021) published a detailed method to culture apical-out chicken organoids. These apical-out organoids are the closest in vitro model to the chicken live intestine but they require live animals for the isolations, they survive only 7 to 9 d in culture, and they reported that there was no postpassage growth or budding of these enteroids (Nash et al., 2021). Apical-out organoids have some advantages in comparison to primary cells, but it should be noted that they can survive only for a relatively short period and they are usually unsuitable for large or long-term screening studies or routine cultures. Indeed, the major limitation of using chicken primary cells or organoids are the short lifespan or the required expensive reagents. cIEC-H2 in contrast has been passaged up to 40 passages at the moment of publication, and, as shown by the reported growth curve and supplementary data, they can stay 15 to 20 d in culture without any major change using basic cell culture reagents and materials. On the other hand, an enterocyte immortalized cell line such as cIEC-H2 lacks the multicellular composition of the in vivo intestine that is more resembled on organoids. This aspect should be carefully considered when choosing a particular intestinal model to perform a study. cIEC-H2 cell line has been immortalized transducing the SV40 Large-T antigen. The immortalization process had not effects on chromosomes number. cIEC-H2 showed the presence of 39 chromosomes with macro- and microdistribution similar to the normal chicken karyotype (Borgaonkar, 1969). Analyzing the mRNA expression of some cell-cycle genes, it is possible to note that the immortalization process mediated by the Large-T antigen has significantly downregulated *RB1* (pRB), *TP53* (p53), *CDKN1A* (p21), cyclin-D1, and cyclin-E1. This is a common effect of SV40 immortalization, as already deeply analyzed by Ahuja and colleagues in their review (Ahuja et al., 2005). Interestingly, *c-MYC* mRNA expression was significantly upregulated on immortalized cIEC-H2 compared to primary cIEC. This upregulation seems to be crucial to regulate cell-cycle progression (Mateyak et al., 1999). Interestingly, also cyclin-D1, a key positive regulator of cell-cycle, was downregulated. Pusch et al. (1996) demonstrated that specific transforming events, such as loss of functional *RB1*, overexpression of c-MYC, can cause transcriptional downregulation of cyclin-D1 expression in logarithmically growing cells (Pusch et al., 1996). Moreover, according to Kim and colleagues (2001), *c-MYC* overexpression may also mediate the downregulation of *CDKN1A* to overcome crisis for Large-T immortalization (Kim et al., 2001). However, the full Large-T immortalization mechanism has not been completely clarified, due to the complexity of cell-cycle regulations during the immortalization phases. cIEC-H2 cell line has been established starting from primary cIEC and these immortalized cells express all the markers typical of enterocytes such as *KRT20, CDH1, EPCAM, SUC-2, MAGM, ALPi* and tight junctions as the freshly isolated counterpart. After a post-confluence differentiation for 48 h using mEGF, the gene expression of some of those markers was upregulated and the cells showed the typical epithelial morphology and characteristics in the immunofluorescence assay. The differentiation process increased the *CDH1* mRNA expression which is a protein directly connected to enterocyte differentiation and crucial for intestinal homeostasis in vivo (Schneider et al., 2010). The same thing happened to *KRT20* and *EPCAM*, with an increase in gene expression that could be correlated to an increase in absorptive differentiation (Zhou et al., 2003; Schnell et al., 2013). Moreover, this hypothesis could be confirmed also comparing the same markers with primary cIEC where those were less expressed than in mEGF differentiated cIEC-H2. However, against expectations, cIEC-H2 were positive for *VIM* in qPCR and IF before differentiation. Typically, *VIM* expression may suggest an onset of epithelial-mesenchymal transition (**EMT**), but since other epithelial proteins' mRNA, such as *CDH1* or *EPCAM* were not downregulated, an EMT of cIEC-H2 can be excluded (Zakrzewski et al., 2013). This phenomenon also appeared in other immortalized epithelial cell lines such as IPEC-J2 (Zakrzewski et al., 2013), MDCK-C7 (Stumpff et al., 2011), or MDBK (Ben-Ze'ev, 1984). Moreover, after the differentiation process the *VIM* mRNA expression was upregulated but

qPCR expression, 6 h after challenge. Data are reported as fold change calculated using the ΔΔCT method. RNA samples with a 260/280 ratio below 2.0 were excluded from the analysis. Outliers were defined by the ROUT Method with the False Discovery Rate (Q) set >1% and excluded from the analysis. Data were normally distributed (Shapiro−Wilk test $P > 0.05$) and they were analyzed using a one-way ANOVA with Tukey's multiple comparisons. IL1B: *CTR* vs. *LPS1* $P = 0.0173$, 95% CI −3.190 to −0.3271, *CTR* vs. *LPS30* $P = 0.0454$, 95% CI −2.045 to −0.02134—IL6: *CTR* vs. *LPS1* $P = 0.0468$, 95% CI −2.286 to −0.01805, *CTR* vs. *LPS30* $P = 0.0282$, 95% CI −1.943 to −0.1250—IL8: *CTR* vs. *LPS30* $P = 0.0021$, 95% CI −19.56 to −5.409− IL10: *CTR* vs. *LPS30* $P = 0.0199$, 95% CI 0.1098−1.145, *LPS1* vs. *LPS30* $P = 0.0027$, 95% CI 0.4602−1.769—TLR4: *CTR* vs. *LPS30* $P = 0.0133$, 95% CI 0.1578−1.264, *LPS1* vs. *LPS30* $P = 0.0087$, 95% CI 0.2951−1.859. Data are represented as mean with SEM ($n = 6$).

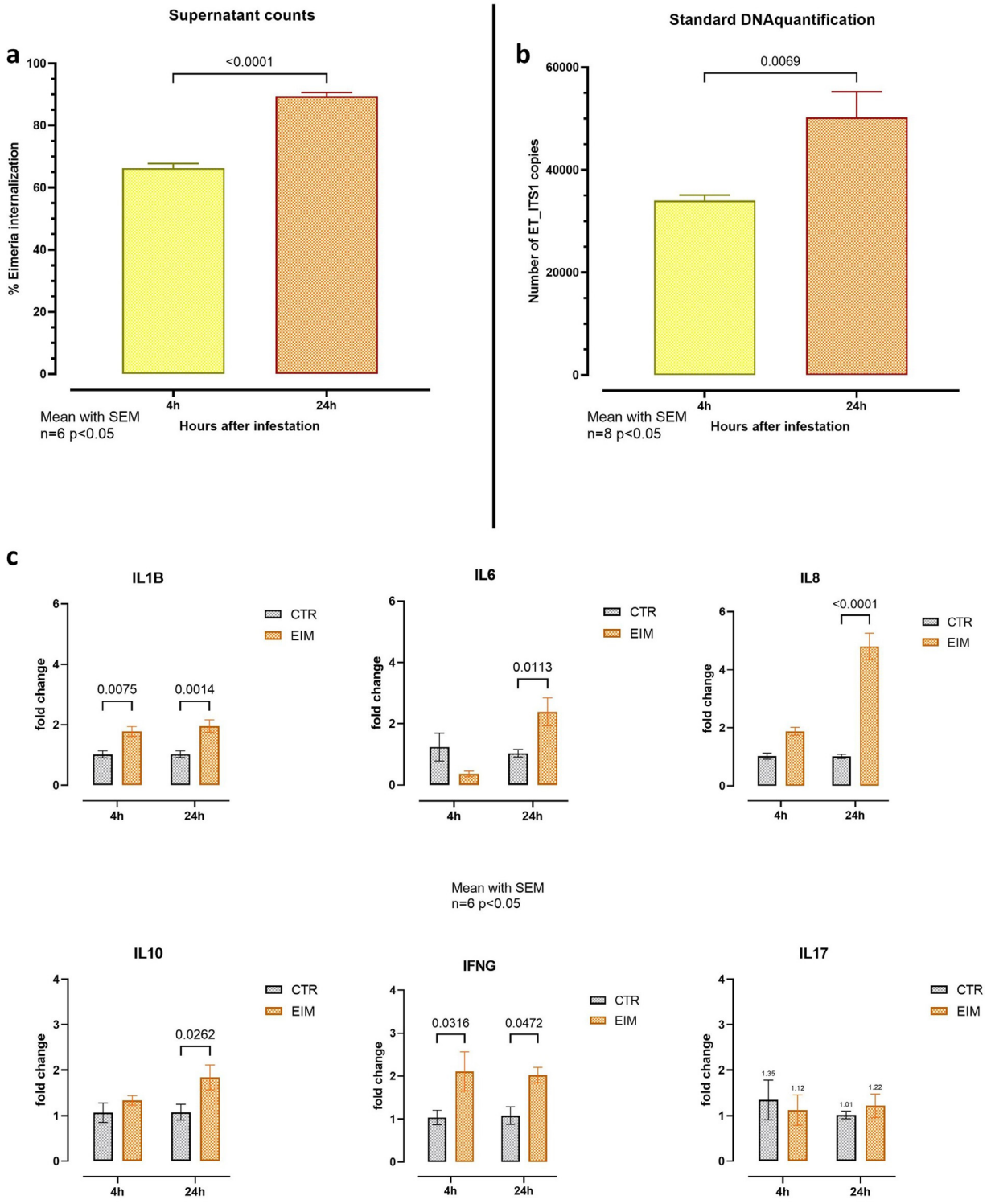

Figure 10. Effect of *Eimeria tenella* invasion on cIEC-H2 passage 4. (a) Invasion efficiency percentage based on sporozoites counted in the supernatant after 4 and 24 h. Outliers were defined by the ROUT Method with the False Discovery Rate (Q) set >1% and excluded from the analysis. Data were normally distributed (Shapiro−Wilk test $P > 0.05$) and analyzed using a 2-tailed unpaired t test $P < 0.0001$; 95% CI 18.35−27.40; t = 12.22, DF = 10. Data are represented as mean with SEM ($n = 6$). (b) Number of copies of *ITS-1* gene based on qPCR standard DNA quantification to detect *Eimeria* inside cells. DNA samples with a 260/280 ratio below 1.8 were excluded from the analysis. Outliers were defined by the ROUT Method with the False Discovery Rate (Q) set >1% and excluded from the analysis. Data were normally distributed (Shapiro−Wilk test $P > 0.05$) and they were analyzed using a 2-tailed unpaired t test $P = 0.0069$; 95% CI 5,223−27,214; t = 3.164, DF = 14. Data are represented as mean with SEM ($n = 8$) and represent 2 technical replicates for each sample. (c) Effect of challenge on innate immune response makers qPCR expression, 4 h and 24 h after challenge. Data are reported as fold change calculated using the ΔΔCT method. RNA samples with a 260/280 ratio below 2.0 were excluded from the analysis. Outliers were defined by the ROUT Method with the False Discovery Rate (Q) set >1% and excluded from the analysis. Data were normally distributed (Shapiro−Wilk test $P > 0.05$) and analyzed using a mixed-effects analysis ($P < 0.05$) with Šídák's multiple comparisons tests. IL1B 4 h: $P = 0.0075$, 95% CI of diff. −1.313 to −0.2020, Predicted (LS) mean diff. −0.7572 t = 3.326, DF = 18.00; 24 h: $P = 0.0014$, 95% CI of diff. −1.486 to −0.3755, Predicted (LS) mean diff. −0.9308, t = 4.088, DF = 18.00—IL6 24 h: $P = 0.0113$, 95% CI of diff. −2.394 to −0.3077, Predicted (LS) mean diff. −1.351, t = 3.194, DF = 16.00—IL8 24 h: $P < 0.0001$, 95% CI of diff. −4.644 to −2.943, Predicted (LS) mean diff. −3.794, t = 10.83, DF = 19.00—IL10 24 h: $P = 0.0262$, 95% CI of diff. −1.428 to −0.08695,

cells were found to be negative in IF. Rusu and colleagues (2005) observed similar behavior in bovine primary jejunocytes with the *VIM* gene expressed but the protein absent in the western blot. This phenomenon was attributed to a suppression of post-transcriptional inhibition of the vimentin synthesis (Rusu et al., 2005).

In studies regarding intestinal health and host−pathogen interactions, the possibility to measure TEER for a prolonged time is a key aspect. After immortalization and 20 d on Transwell supports cIEC-H2 TEER values remained as low as primary cIEC, around 40 to 50 Ω^*cm^2. Probably, the characteristics of primary chicken enterocytes obtained with the isolation method and then used to generate the cIEC-H2 cell line do not allow a higher TEER value. This could be considered a drawback, but also with these low values, the effect of inflammatory challenge on TEER values was still visible. Typically, human epithelial cells (such as Caco-2) used as barrier models can reach a TEER value of 200 to 300 Ω^*cm^2 (Natoli et al., 2012); though the chicken intestine behaves differently, presenting average TEER values between 20 to 40 and 100 to 200 Ω^*cm^2, from the jejunum to the rectum (Amat et al., 1999; Bialkowski et al., 2023).

In this study, cIEC-H2 were also functionally characterized. This cell line showed ALP activity around 50 mU/L similarly to primary cIEC, and the ability to create an innate immune response with the positive expression and upregulation of *IL1B, IL6*, and *IL8* when exposed to a pro-inflammatory stimulus. Moreover, these cells also responded to *E. tenella* sporozoites' invasion. *E. tenella* sporozoites need to invade epithelial cells to complete their endogenous lifecycle. In vitro, MDBK or other mammalian cells are usually used as a continuous cell model to assess invasion efficiency (Felici et al., 2021). However, to our knowledge, those cells have never been successfully used to detect cytokine gene expression. cIEC-H2 cells were able to respond to *E. tenella* infection by upregulating *IL1B, IL6, IFNG,* and *IL8*, consistently to what was seen in vivo (Laurent et al., 2001; Cornelissen et al., 2009; Yu et al., 2021). Furthermore, in 2018, Bussière and colleagues published a work where chicken lung epithelial cell line (**CLEC-213**) were used to develop a new model to study *E. tenella* gametogony in vitro (Bussière et al., 2018). They used CLEC-213 due to the absence of a characterized avian intestinal or cecal epithelial cell line. Moreover, they failed to demonstrate gametogony of wild-type *E. tenella* due to the difficulties in maintaining CLEC-213 in culture for 7 d (Bussière et al., 2018). The use of cIEC-H2 as intestinal host-specific cell line would allow better characterization of coccidiosis pathogenesis, and the study of new strategies of intervention without the limitations and costs of primary cells or organoids. Together with coccidia, these cells could also help the study of specific chicken pathogens in vitro, to find solutions against common threats such as *Salmonella spp., C. perfringens*, or *Campylobacter spp.*, and viruses that could also result harmful to human health (CDC, 2022).

In conclusion, in this study, an immortalized chicken enterocytes cell line was successfully developed and characterized. These cells could become a useful model to study intestinal health and all the interactions with chicken intestinal pathogens in vitro. Moreover, they guarantee a cost-effective and easy-to-maintain model for all the public health, food safety, or research laboratories that study chicken intestinal epithelium and chicken cells in health and disease.

ACKNOWLEDGMENTS

This work was supported by a grant from Vetagro S.p.A. (Reggio Emilia, Italy). Funders participated in the study design, collection, analysis, interpretation of data, and writing of the manuscript.

DISCLOSURES

The authors declare the following financial interests/personal relationships which may be considered as potential competing interests: Ester Grilli reports financial support was provided by Vetagro S.p.A. Andrea Piva reports a relationship with Vetagro S.p.A. that includes: board membership. Andrea Piva reports a relationship with University of Bologna that includes: employment. Ester Grilli reports a relationship with Vetagro Inc. that includes: board membership. Ester Grilli reports a relationship with University of Bologna that includes: employment.

SUPPLEMENTARY MATERIALS

Supplementary material associated with this article can be found in the online version at doi:10.1016/j.psj.2023.102864.

REFERENCES

Ahuja, D., M. T. Sáenz-Robles, and J. M. Pipas. 2005. SV40 large T antigen targets multiple cellular pathways to elicit cellular transformation. Oncogene 24:7729–7745.

Ali, A., R. Kolenda, M. M. Khan, J. Weinreich, G. Li, L. H. Wieler, K. Tedin, and D. Roggenbuck. 2020. Novel avian pathogenic escherichia coli genes responsible for adhesion to chicken and human cell lines. Appl. Environ. Microbiol. 86:e01068–20.

Amat, C., J. Piqueras, J. Planas, and M. Moreto. 1999. Electrical properties of the intestinal mucosa of the chicken and the effects of luminal glucose. Poult. Sci. 78:1126–1131.

Bar Shira, E., and A. Friedman. 2018. Innate immune functions of avian intestinal epithelial cells: response to bacterial stimuli and localization of responding cells in the developing avian digestive tract. PLoS One 13:e0200393.

Predicted (LS) mean diff. −0.7574, t = 2.786, DF = 16.00—IFNG 4 h: $P = 0.0316$, 95% CI of diff. −2.084 to −0.0931, Predicted (LS) mean diff. −1.088, t = 2.716, DF = 15.00; 24 h: $P = 0.0472$, 95% CI of diff. −1.925 to −0.01122, Predicted (LS) mean diff. −0.9679, t = 2.513, DF = 15.00. Data are represented as mean with SEM ($n = 6$). Abbreviations: CTR, control group; EIM, *E. tenella* 1×10^5 sporozoites; *IFNG*, interferon gamma; IL, interleukin. ITS-1, *E. tenella* internal transcribed spacer-1.

Ben-Ze'ev, A. 1984. Differential control of cytokeratins and vimentin synthesis by cell-cell contact and cell spreading in cultured epithelial cells. J. Cell Biol. 99:1424–1433.

Bialkowski, S., A. Toschi, L. Yu, L. Schlitzkus, P. Mann, E. Grilli, and Y. Li. 2023. Effects of microencapsulated blend of organic acids and botanicals on growth performance, intestinal barrier function, inflammatory cytokines, and endocannabinoid system gene expression in broiler chickens. Poult. Sci. 102:102460.

Borgaonkar, D. S. 1969. Observations on the chromosomes of one chicken (Gallus domesticus). Poult. Sci. 48:331–333.

Bussière, F. I., A. Niepceron, A. Sausset, E. Esnault, A. Silvestre, R. A. Walker, N. C. Smith, P. Quéré, and F. Laurent. 2018. Establishment of an in vitro chicken epithelial cell line model to investigate *Eimeria tenella* gamete development. Parasit. Vectors 11:44.

Byrne, C. M., M. Clyne, and B. Bourke. 2007. *Campylobacter jejuni* adhere to and invade chicken intestinal epithelial cells in vitro. Microbiology 153:561–569.

CDC. 2022. Chicken and food poisoning. Centers for Disease Control and Prevention. https://www.cdc.gov/foodsafety/chicken.html. Accessed January 14, 2023.

Cornelissen, J. B. W. J., W. J. C. Swinkels, W. A. Boersma, and J. M. J. Rebel. 2009. Host response to simultaneous infections with *Eimeria acervulina, maxima* and *tenella*: a cumulation of single responses. Vet. Parasitol. 162:58–66.

Dimier-Poisson, I. H., D. T. Bout, and P. Quéré. 2004. Chicken primary enterocytes: inhibition of *Eimeria tenella* replication after activation with crude interferon-γ supernatants. Avian Dis. 48:617–624.

FAOSTAT. (2018) http://www.fao.org/faostat/en/?#data/. Accessed November 4, 2018.

Felici, M., B. Tugnoli, A. Piva, and E. Grilli. 2021. In vitro assessment of anticoccidials: methods and molecules. Anim. Open Access J. 11:1962.

Ghiselli, F., B. Rossi, M. Felici, M. Parigi, G. Tosi, L. Fiorentini, P. Massi, A. Piva, and E. Grilli. 2021a. Isolation, culture, and characterization of chicken intestinal epithelial cells. BMC Mol. Cell Biol. 22:12.

Ghiselli, F., B. Rossi, A. Piva, and E. Grilli. 2021b. Assessing intestinal health. In vitro and ex vivo gut barrier models of farm animals: benefits and limitations. Front. Vet. Sci 8:723387.

Guo, S., C. Li, D. Liu, and Y. Guo. 2015. Inflammatory responses to a *Clostridium perfringens* type A strain and α -toxin in primary intestinal epithelial cells of chicken embryos. Avian Pathol. 44:81–91.

Han, X., and L. D. Bertzbach. 2019. Mimicking the passage of avian influenza viruses through the gastrointestinal tract of chickens. Vet. Microbiol. 239:108462.

Immerseel, F. V., J. D. Buck, I. D. Smet, F. Pasmans, F. Haesebrouck, and R. Ducatelle. 2004. Interactions of butyric acid− and acetic acid−treated *Salmonella* with chicken primary cecal epithelial cells in vitro. Avian Dis. 48:384–391.

John, D. A., L. K. Williams, V. Kanamarlapudi, and T. J. Humphrey. 2017. The bacterial species campylobacter jejuni Induce diverse innate immune responses in human and avian intestinal epithelial cells. Front. Microbiol. 8:1840.

Kaiser, A., T. Willer, P. Steinberg, and S. Rautenschlein. 2017. Establishment of an in vitro intestinal epithelial cell culture model of avian origin. Avian Dis. 61:229–236.

Kawahara, F., K. Taira, S. Nagai, H. Onaga, M. Onuma, and T. Nunoya. 2008. Detection of five avian *Eimeria* species by species-specific real-time polymerase chain reaction assay. Avian Dis. 52:652–656.

Kim, H.-S., J.-Y. Shin, J.-Y. Yun, D.-K. Ahn, and J.-Y. Lee. 2001. Immortalization of human embryonic fibroblasts by overexpression of c-MYC and simian virus 40 large T antigen. Exp. Mol. Med. 33:293–298.

Kolenda, R., M. Burdukiewicz, M. Wimoné, A. Aleksandrowicz, A. Ali, I. Szabo, K. Tedin, J. Bartholdson Scott, and D. Pickard. 2021. Identification of natural mutations responsible for altered infection phenotypes of salmonella enterica clinical isolates by using cell line infection screens. Appl. Environ. Microbiol. 87:e02177–20.

Laurent, F., R. Mancassola, S. Lacroix, R. Menezes, and M. Naciri. 2001. Analysis of chicken mucosal immune response to *Eimeria tenella* and *Eimeria maxima* infection by quantitative reverse transcription-PCR. Infect. Immun. 69:2527–2534.

Li, J., J. Li, S. Y. Zhang, R. X. Li, X. Lin, Y. L. Mi, and C. Q. Zhang. 2018. Culture and characterization of chicken small intestinal crypts. Poult. Sci. 97:1536–1543.

Livak, K. J., and T. D. Schmittgen. 2001. Analysis of relative gene expression data using real-time quantitative PCR and the 2(-Delta Delta C(T)) Method. Methods San Diego Calif. 25:402–408.

Manfredi, J. J., and C. Prives. 1994. The transforming activity of simian virus 40 large tumor antigen. Biochim. Biophys. Acta 1198:65–83.

Mateyak, M. K., A. J. Obaya, and J. M. Sedivy. 1999. c-MYC regulates cyclin D-CDK4 and -CDK6 activity but affects cell cycle progression at multiple independent points. Mol. Cell. Biol. 19:4672–4683.

Maynard, C. L., C. O. Elson, R. D. Hatton, and C. T. Weaver. 2012. Reciprocal interactions of the intestinal microbiota and immune system. Nature 489:231–241.

Nash, T. J., K. M. Morris, N. A. Mabbott, and L. Vervelde. 2021. Inside-out chicken enteroids with leukocyte component as a model to study host−pathogen interactions. Commun. Biol. 4:1–15.

Natoli, M., B. D. Leoni, I. D'Agnano, F. Zucco, and A. Felsani. 2012. Good Caco-2 cell culture practices. Toxicol. In Vitro 26:1243–1246.

Oost, M. J., A. Ijaz, D. A. van Haarlem, K. van Summeren, F. C. Velkers, A. D. Kraneveld, K. Venema, C. A. Jansen, R. H. H. Pieters, and J. P. ten Klooster. 2022. Chicken-derived RSPO1 and WNT3 contribute to maintaining longevity of chicken intestinal organoid cultures. Sci. Rep. 12:10563.

Orr, B., K. Sutton, S. Christian, T. Nash, H. Niemann, L. L. Hansen, M. J. McGrew, S. R. Jensen, and L. Vervelde. 2021. Novel chicken two-dimensional intestinal model comprising all key epithelial cell types and a mesenchymal sub-layer. Vet. Res. 52:142.

Pierzchalska, M., M. Grabacka, M. Michalik, K. Zyla, and P. Pierzchalski. 2012. Prostaglandin E2 supports growth of chicken embryo intestinal organoids in Matrigel matrix. Biotechniques 52:307–315.

Pusch, O., T. Soucek, E. Wawra, E. Hengstschläger-Ottnad, G. Bernaschek, and M. Hengstschläger. 1996. Specific transformation abolishes cyclin D1 fluctuation throughout the cell cycle. FEBS Lett. 385:143–148.

Rath, N. C., R. Liyanage, A. Gupta, and B. Packialakshmi. 2018. A method to culture chicken enterocytes and their characterization. Poult. Sci. 97:4040–4047.

Rusu, D., S. Loret, O. Peulen, J. Mainil, and G. Dandrifosse. 2005. Immunochemical, biomolecular and biochemical characterization of bovine epithelial intestinal primocultures. BMC Cell Biol. 6:42.

Schneider, C. A., W. S. Rasband, and K. W. Eliceiri. 2012. NIH Image to ImageJ: 25 years of image analysis. Nat. Methods 9:671–675.

Schneider, M. R., M. Dahlhoff, D. Horst, B. Hirschi, K. Trülzsch, J. Müller-Höcker, R. Vogelmann, M. Allgäuer, M. Gerhard, S. Steininger, E. Wolf, and F. T. Kolligs. 2010. A key role for E-cadherin in intestinal homeostasis and Paneth cell maturation. PLoS One 5:e14325.

Schnell, U., V. Cirulli, and B. N. G. Giepmans. 2013. EpCAM: structure and function in health and disease. Biochim. Biophys. Acta 1828:1989–2001.

Sheppard, H. M., S. I. Corneillie, C. Espiritu, A. Gatti, and X. Liu. 1999. New insights into the mechanism of inhibition of p53 by simian virus 40 large T antigen. Mol. Cell. Biol. 19:2746–2753.

Stumpff, F., M.-I. Georgi, L. Mundhenk, I. Rabbani, M. Fromm, H. Martens, and D. Günzel. 2011. Sheep rumen and omasum primary cultures and source epithelia: barrier function aligns with expression of tight junction proteins. J. Exp. Biol. 214:2871–2882.

Uhlmann, V., R. Delgado-Gonzalo, M. Unser, P. O. Michel, L. Baldi, and F. M. Wurm. 2016. USER-friendly image-based segmentation and analysis of chromosomes. Pages 395−398 in 2016 IEEE 13th International Symposium on Biomedical Imaging (ISBI).

Van De Walle, J., A. Hendrickx, B. Romier, Y. Larondelle, and Y.-J. Schneider. 2010. Inflammatory parameters in Caco-2 cells: effect of stimuli nature, concentration, combination and cell differentiation. Toxicol. In Vitro 24:1441–1449.

Yu, H., W. Zou, C. Mi, Q. Wang, G. Dai, T. Zhang, G. Zhang, K. Xie, J. Wang, and H. Shi. 2021. Research note: expression of T cell-related cytokines in chicken cecal and spleen tissues following *Eimeria tenella* infection in vivo. Poult. Sci. 100:101161.

Yuan, C., Q. He, J. Li, M. M. Azzam, J. Lu, and X. Zou. 2015. Evaluation of embryonic age and the effects of different proteases on the

isolation and primary culture of chicken intestinal epithelial cells in vitro: primary culture of chicken IEC in vitro. Anim. Sci. J. 86:588–594.

Zakrzewski, S. S., J. F. Richter, S. M. Krug, B. Jebautzke, I.-F. M. Lee, J. Rieger, M. Sachtleben, A. Bondzio, J. D. Schulzke, M. Fromm, and D. Günzel. 2013. Improved cell line IPEC-J2, characterized as a model for Porcine Jejunal Epithelium. PLoS ONE 8:e79643.

Zhou, Q., D. M. Toivola, N. Feng, H. B. Greenberg, W. W. Franke, and M. B. Omary. 2003. Keratin 20 helps maintain intermediate filament organization in intestinal epithelia. Mol. Biol. Cell 14:2959–2971.